Investigating the role of papain-like cysteine protease RD21 in plant-pathogen interactions

Inaugural–Dissertation
zur
Erlangung des Doktorgrades
der Mathematisch-Naturwissenschaftlichen Fakultät
der Universität zu Köln

vorgelegt von
Takayuki SHINDO
aus Japan

Köln, April 2009

Die vorliegende Arbeit wurde am Max-Planck-Institut für Züchtungsforschung in Köln erstellt.

Berichterstatter: Prof. Dr. Paul Schulze-Lefert
Prof. Dr. Reinhard Krämer

Prüfungsvorsitzende: Prof. Dr. Ute Höcker

Tag der Disputation: 29. April 2009

CONTENTS

Publications

Shindo, T., and Van der Hoorn, R. A. L. (2008) Papain-like cysteine proteases: key players at molecular battlefields employed by both plants and their invaders. **Mol. Plant Pathol.** 9, 119-125. (some parts were used in introduction)

Shabab*, M., Shindo*, T., Gu, C., Kaschani, F., Pansuriya, T., Chintha, R., Harzen A., Colby, T., Kamoun, S., and Van der Hoorn, R. A. L. (2008) Fungal effector protein AVR2 targets diversifying defence-related Cys proteases of tomato. **Plant Cell** 20, 1169-1183.

Wang*, Z., Gu*, C., Colby, T., Shindo, T., Balamurugan, R., Waldmann, H., Kaiser, M., and Van der Hoorn, R. A. L. (2008) Beta-lactone probes identify a papain-like peptide ligase in *Arabidopsis thaliana*. **Nat. Chem. Biol.** 4, 557-563.

Table of abbreviations

::	fused to (in the context of gene fusion constructs)
%	percent
° C	degree Celsius
3’	three prime end of a DNA fragment
5’	five prime end of a DNA fragment
35S	double 35S promoter of CaMV
avr	avirulence
bp	base pair(s)
BTH	benzo(1,2,3)thiadiazole-7-carbothioic acid S-methyl ester
CaMV	cauliflower mosaic virus
cDNA	complementary DNA
cfu	colony forming unit
Col-0	*Arabidopsis thaliana* ecotype *Columbia*
d	day(s)
dH_2O	deionised water
DMSO	dimethylsulfoxide
DNA	deoxyribonucleic acid
dNTP	deoxynucleosidetriphosphate
dpi	days post infiltration
DTT	dithiothreitol
E-64	(2S,3S)-3-(N-{(S)-1-[N-(4-guanidinobutyl)carbamoyl]3-methylbutyl}carbamoyl) oxirane-2-carboxylic acid
EDTA	ethylenediaminetetraacetic acid
Emwa1	*Hyaloperonospora parasitica* isolate Emwa1
Fig.	Figure
g	gram
g	gravity constant (9.81 ms^{-1})
GFP	Green fluorescent protein
h	hour(s)
hp	hairpin-like structured
HR	hypersensitive response
HRP	horseradish peroxidase
kb	kilobase(s)
kDa	kiloDalton(s)
l	litre

Ler	*Arabidopsis thaliana* ecotype *Landsberg erecta*
m	milli
M	molar (mol/l)
µ	micro
min	minute(s)
mM	millimolar
N	amino-terminal
Noco2	*Hyaloperonospora parasitica* isolate Noco2
OD^{600}	optical density
PAD3	Phytoalexin Deficient 3
PCR	polymerase chain reaction
PAGE	polyacrylamide gel-electrophoresis
pH	negative decimal logarithm of the H^+ concentration
PR	pathogenesis related
Pst	*Pseudomonas syringae* pv. *tomato*
pv.	Pathovar
PVX	Potato Virus X
R	resistance
RNA	ribonucleic acid
RNAi	double-stranded RNA interference
rpm	rounds per minute
RT-PCR	reverse transcription-polymerase chain reaction
SA	salicylic acid
SGT1	Suppressor of G-Two allele of Skp1
SID2	Salicylic Acid Induction–Deficient 2
SDS	sodium dodecyl sulphate
sec	second(s)
TBS	Tris buffered saline
T-DNA	transfer DNA
TMV	Tobacco mosaic virus
TRV	Tobacco Rattle Virus
VIGS	virus-induced gene silencing
Vir	virulence
Ws	*Arabidopsis thaliana* ecotype Wassilewskija
WT	wild-type

Abstract

DCG-04 is a biotinylated derivative of cysteine protease inhibitor E-64, which irreversibly reacts with papain-like cysteine proteases (PLCPs) when these proteases are active. Using DCG-04, seven active proteases are labelled in *Arabidopsis* leaf extracts. Of these, RD21 (responsive to desiccation-21) was found to have increased activity during the infection with avirulent *Pseudomonas syringe* in Arabidopsis cell cultures. Infection with a virulent strain caused post-translational suppression of RD21 activity. These data suggest that RD21A plays a role in defence. We therefore challenged single, double and triple knock-out lines of RD21-like proteases with several pathogens and detected an altered susceptibility for *Botrytis cinerea*, but not the other pathogens tested. Presumably because adapted pathogens might use inhibitors that make them insensitive for RD21A.

As an alternative reverse genetic approach, we silenced the RD21 orthologs of *Nicotiana benthamiana* using virus-induced gene silencing with Tobacco Rattle Virus (TRV)-based silencing vectors. *NbRd21* silencing resulted in retarded growth and spreading cell death, most likely triggered by a combination of *NbRd21* silencing and TRV presence. Interestingly, silencing of autophagy-related genes, *ATG3* and *ATG6*, pheno-copied *NbRD21* silencing. Furthermore, DCG-04 activity profiling assay showed the suppression of NbRD21 activity and up-regulation of *NbRd21* transcript in ATG3 (and ATG6) silenced plants, which implies a connection between RD21, cell death and autophagy.

To identify other defence-related PLCPs, we applied benzothiadiazole (BTH) to trigger the salicylic acid–regulated defence pathway in tomato. Of the seven PLCPs tested, transcription of only *PIP1* and *RCR3* were induced. Sequencing of PLCP alleles of tomato relatives revealed that same proteases, PIP1 and RCR3, are under diversifying selection, resulting in variant residues around the substrate binding groove. Taken together these data indicate that some PLCPs are involved in plant-pathogen interactions.

Zusammenfassung

DCG04 ist ein biotinyliertes Derivat des Cysteinprotease Hemmstoffs E-64, welcher irreversible mit papainähnlichen Cysteinproteasen (PLCPs) reagiert, wenn diese in aktiver Form vorliegen. DCG-04 markiert sieben aktive Proteasen in *Arabidopsis* Blattextrakten Eine dieser Proteasen, RD21 (Responsive to Desiccation-21), weist eine erhöhte Aktivität während einer avirulent *Pseudomonas syringae*-Infektion in *Arabidopsis*- Zellkulturen auf. Eine Infektion mit einem virulenten *Pseudomonas* Stamm führte hingegen zu einer post- translationalen Unterdrückung der RD21 Aktivität, was vermuten lässt, dass RD21 eine Rolle in der Pathogenabwehr spielt. Um diese Vermutung zu belegen, haben wir Einfach-, Doppel-und Dreifach-Knockoutmutanten der RD21- ähnlichen granulierten Proteasen verschiedenen Pathogenen ausgesetzt. Dabei stellten wir fest, dass sich unter diesen Bedingungen nur die Anfälligkeit gegenüber *Botrytis cinerea* verändert hat, vermutlich weil angepasste Pathogene Hemmstoffe nutzen, um gegenüber RD21 weniger anfällig zu sein.

Um die Rolle von RD21 in *N. benthamiana* zu klären, haben wir die genetisch-rückwärtsgerichtete Methode des Virus- induzierten Silencing (VIGS) mit auf dem Tobacco Rattle Virus (TRV)-basierenden silencing Vektoren von RD21-orthologen Genen durchgeführt. Dabei konnten wir beobachten, dass das Unterdrücken von *NbRD21* zu unterentwickeltem Wuchs und sich ausbreitendem Zelltod führt, und vermuten, dass diese Reaktion höchstwahrscheinlich durch eine Kombination von RD21A-Unterdrückung und dem Vorhandensein des Silencing-Vektor TRV ausgelöst wurde. Interessanterweise hat das Unterdrücken der Gene ATG3 und ATG6, die eine Rolle bei der Autophagie spielen, den gleichen Einfluss auf die phenotypische Entwicklung von *Nb* wie das Silencing von RD21. Zusätzlich konnte anhand von aktivitätsbezogenen Untersuchungen mit DCG04 einen eine klare Verminderung des RD21-Signals in Pflanzen, in denen die Expression von *ATG3* und *ATG6* unterdrückt ist, nachgewiesen werden, wobei das Transkriptionslevel der Cysteinprotease erhöht ist. Diese Ergebnisse stützen die Annahme, dass ein deutlicher Zusammenhang zwischen NbRd21, Zelltod und Autophagie besteht.

Um darüberhinaus weitere abwehrverwandten PLCPs zu identifizieren, nutzen wir Benzothiadiazol (BTH), um den Salizylsäure-regulierten Abwehrmechanismus in Tomate einzuleitet. Von sieben getesteten PLCPs wurde nur die Transkription von PIP1 und RCR3 induziert. Die Sequenzierung von PLCP-Allelen verwandter Species zeigte, dass diese Proteasen, PIP1 und RCR3 unter Selektionsdruck stehen, was sich im Auftreten unterschiedlicher Aminosäuren um die Substratbindestelle herum

wiederspiegelt. Letztlich weisen diese Ergebnisse stark daraufhin, dass einige PLCPs eine Rolle in Pflanzen-Pathogen Interaktionen besitzen

1 Introduction

In all organisms, non-functional proteins are degraded into amino acids by proteases. Some proteases, however, are more selective and play key roles in signalling cascades, regulating defence responses and during development (Van der Hoorn, 2008). Proteases are grouped into four classes based on the active site nucleophile used; cysteine, serine, methallo- or aspartic proteases.

1.1. Classification and structure of papain-like cysteine proteases

Proteases are grouped into families and clans in the MEROPS database based on structural and evolutionary criteria (http://merops.sanger.ac.uk/, Rawlings *et al*., 2008). To date, 70 families belonging to 12 different clans are cysteine proteases (Salas *et al*., 2008). Family C1 (Cysteine protease 1) is subdivided into C1A and C1B. C1A family members carry a signal peptide for the secretion and contain disulfide bridges. Whereas, C1B family members are localised in the cytoplasm and do not contain disulfide bridges (Rawlings *et al*., 2006). Plants only have C1A subfamily proteases (Van der Hoorn, 2008). Papain-like cysteine proteases (PLCPs) belong to the family C1 of clan CA. PLCPs show the typical papain-like fold described by Drenth *et al*. (1968); two domains, an α-helix-rich domain and a β-barrel-like domain, separating a substrate-binding grove containing the active site (Figure 1.1.A). PLCPs are 23-30 kDa in size and cleave peptide bonds of protein substrates using a catalytic cysteine residue as a nucleophile. PLCPs are produced with an N-terminal auto-inhibitory domain (called prodomain) which covers the substrate binding groove and needs to be proteolytically removed for protease activation (Figure 1.1.B) (Taylor *et al*., 1995). The actual auto-inhibitory motif in the prodomain is the conserved ERFNIN motif (Grudkowska and Zagdanska, 2004). Some proteases carry a vacuolar targeting signal (NPIR) in the prodomain and a predicted endoplasmic reticulum protein retention signal (KDEL) at C-terminus (Grudkowska and Zagdanska, 2004).

1.2. PLCPs in plants

In Arabidopsis there are ~30 genes encoding PLCPs which can be subdivided into 8 of subfamilies based on the phylogenetic similarities (Figure 1.2) (Beers *et al*., 2004). To date only few have been studied in detail. These include SAG12, AALP and XCP2 are described below.

SAG12 (*Senescence-Associated Gene 12*) is a well known senescence-marker since its transcript level is up-regulated upon senescence and drought stress (Lohman *et al*., 1994). Senescence specific regulation of *SAG12* is tightly controlled by a highly

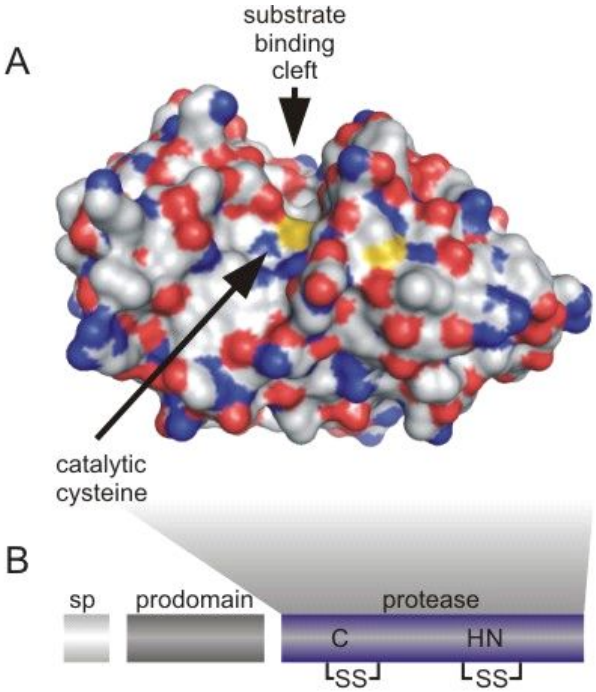

Fig. 1.1 Characteristics of papain-like cysteine proteases

A) Surface representation of the crystal structure of papain, showing its wide substrate binding cleft with the catalytic cysteine (yellow).

B) Domain structure of open reading frame of PLCPs of family C1A. The signal peptide (sp) targets the protein to the endomembrane system; the autoinhibitory prodomain needs to be removed to activate the protease. The protease domain contains three catalytic residues: cysteine (C), histidine (H) and asparagine (N), and often contains two disulphide bridges (SS).

conserved region of the SAG12 promoter (Noh and Amasino, 1999A, B). SAG12 is localised in acidic senescence-associated vacuoles. During senescence, cells containing these vacuoles shows the expression of *SAG12* (Otegui *et al*., 2004). However, *sag12* Arabidopsis mutants did not develop a phenotype under normal growth conditions and during senescence (Otegui *et al*., 2004). This suggests that SAG12 is functionally redundant with other proteases.

AALP (*Arabidopsis Aleurain-Like Protease*) is highly homologous to the barley aleurain protease and is a well-known vacuolar marker protein (Ahmed *et al.*, 2000). In barley, this cysteine protease is synthesized in the endoplasmic reticulum and transported through the Golgi to vacuole (Ahmed *et al.*, 2000). Processing occurs before the proprotease reaches the acidic compartment of cells and includes two steps; a clipping step to remove prodomain and a trimming step to remove a small peptide (Holwerda *et al.*, 1990). The clipping step might require the activity of another cysteine protease, called RD21 (see below for details) (Halls *et al.*, 2005). Co-incubation of proAALP with protease RD21 caused clipping and protease maturation (Halls *et al.*, 2005). A number of phenotypes have been reported for AALP. Suppression of transcript levels of aleurain-like protease in *Brassica oleracea*, BoCP5, delays senescence (Eason *et al.*, 2005). *Colletotrichum destructivum* inoculation to *N. benthamiana* increases the expression of AALP ortholog *NbCYP1* and *NbCYP1* silenced plants were more susceptible (Hao *et al.*, 2006). To date, no more Arabidopsis *aalp* mutant phenotype has been reported.

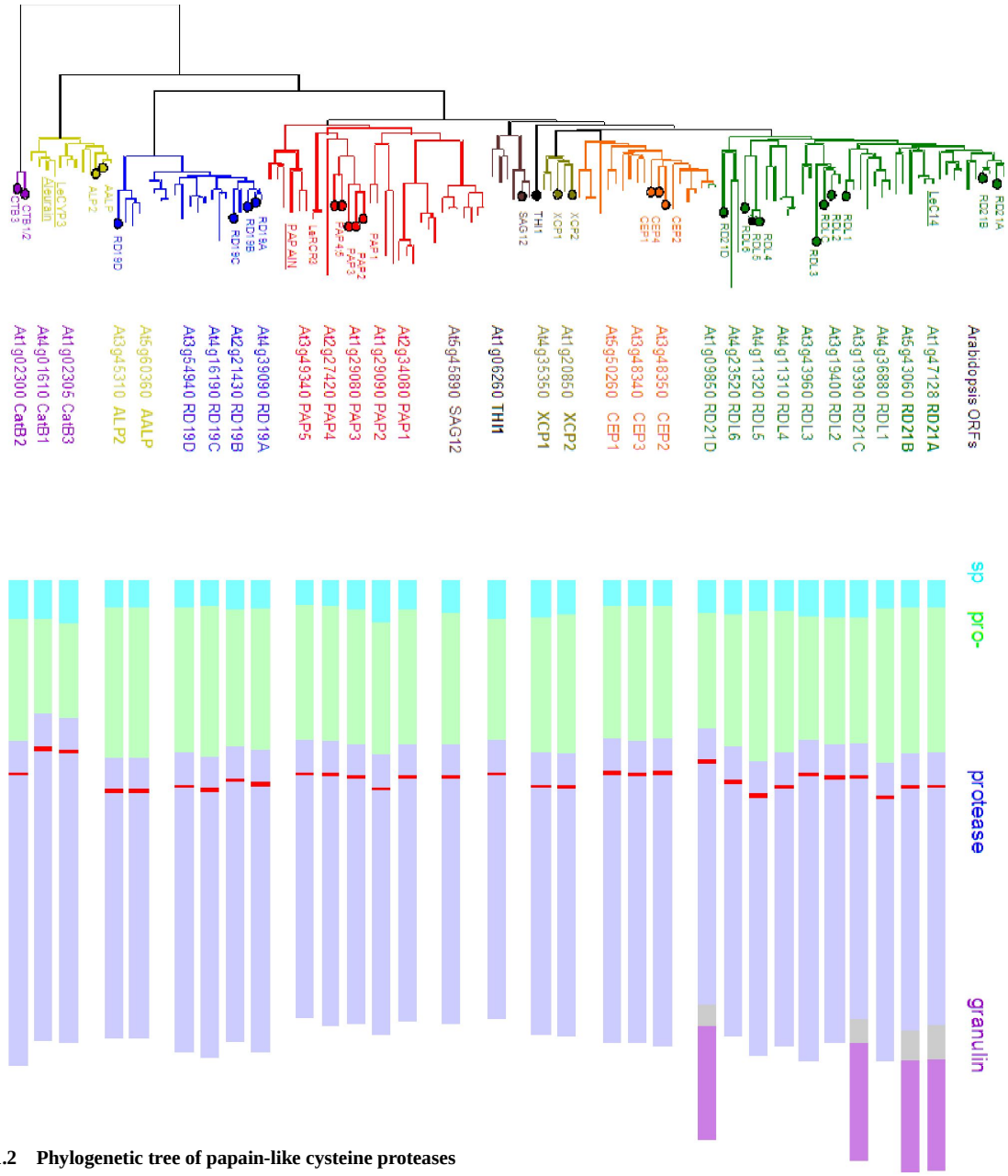

Fig. 1.2 Phylogenetic tree of papain-like cysteine proteases

Based on the phylogenetic similarities, plant PLCPs are subdivided into 8 subfamilies (colors in phylogenetic tree). The 31 Arabidopsis PLCPs are indicated with dots and protein domains are shown on the right. Sp, Signal peptide; Pro-, N-terminal pro-domain; Protease, protease domain, with catalytic Cys (red); granulin, C-terminal granulin domain. The Gray region between the protease and granulin is the proline-rich domain. Names with under line represents PLCP encoded from other plant species. This phylogenetic tree is adapted and redrawn from Beers *et al*. (2004).

XCP1 and ***XCP2*** (**Xylem cysteine proteases**) are two paralogs in Arabidopsis which encode proteins sharing 70% identity (Beers *et al.*, 2004). These genes are highly expressed in flowers and stems, in particular in xylem but not in bark (Zhao *et al.*, 2000). XCP1 and XCP2 proteins are transported to the central vacuole of trachery elements

during secondary cell wall thickening, suggesting XCPs are involved in autolysis of trachery elements (Funk *et al.*, 2002, Avci *et al.*, 2008). Interestingly, recombinant XCP1 becames only active at pH 5.5 and also the XCP homologue Tr-cp14 in white clover (*Trifolium repens*) is activated at pH 5 (Zhao *et al.*, 2000, Asp *et al.*, 2004). Ectopically expressed XCP1 *in planta* resulted in a reduction in plant size and early leaf senescence phenotype (Funk *et al.*, 2002). *xcp1xcp2* double knock-out plants showed a delay in clearing cellular remnants in vacuoles during autolysis (Avci *et al.*, 2008). This indicates that XCPs play a role as degrading enzymes in the xylem cells during autolysis.

In short, PLCPs show a tight connection to plant senescence, probably due to their role as degrading enzymes. But some PLCPs possess a specialised function in plants.

1.3. Plant PLCPs acting extracellular defence

Plants use PLCPs to protect themselves against pests and pathogen attack. Examples are papain from papaya and Mir1 from maize, both acting against insect larvae. Tomato RCR3 and PIP1 are induced upon pathogen attack and inhibited by pathogen-derived inhibitors. Arabidopsis RD19 is required for resistance against bacterial pathogens. *N. benthamiana* CatB contributes to the defence response. These PLCPs are described below.

Papain is a component of latex of papaya trees, which pours out of wounds, presumably as a defence response against herbivores (reviewed by El Moussaoui *et al.*, 2001). The structure of papain was one of the earliest resolved protein structures (Drenth *et al.*, 1968). Papain is produced as a preproprotein, and mechanical wounding of papaya fruit enhances papain accumulation and activation (Moutim *et al.*, 1999; Azarkan *et al*., 2006). However, the mechanism of its accumulation and how it is activated is not clear, yet. A role of papain in insect defence has been described only recently. Different lepidopteran caterpillars (*Samia ricini*, *Mamestra brassicae* and *Spodoptera litura*) had reduced larval weight when fed with leaves containing papain (Konno *et al*., 2004). This reduced growth was not the case when the latex was washed out or when the leaves were treated with the cysteine protease inhibitor E-64 (Konno *et al*., 2004). This indicates that papain contributes to defence against herbivores.

Mir1 (*Maize imbred resistance 1*) was identified because it was encoded by an abundant transcript in callus of resistant but not susceptible maize when challenged with armyworms (*Spodoptera fugiperda*) (Jiang *et al*., 1995; Pechan *et al*., 1999). Like papain, Mir1 is translated as a preproprotein, suggesting that it is secreted or localized

to vesicles. Mir1 protein accumulation occurs rapidly one hour after larval feeding, continues for seven days and is most abundant at the feeding site (Pechan *et al*., 2000). Tobacco budworm (*Heliothis virescens*) larvae fed with transgenic maize callus over expressing the *Mir1* gene were significantly smaller than those fed with callus from control plants (Pechan *et al*., 2000; Chang *et al*., 2000). Feeding on resistant or *Mir1* transgenic plants causes severe damage of the caterpillar peritorophic matrix, which is the chitin structure covering the insect gut surface, protecting it from chemical and physical damage (Pechan *et al*., 2002). It has been suggested that Mir1 can bind to chitin, localizing the proteolytic activity to the insect gut (Pechan *et al*., 2002).

PIP1 (*Phytophthora* inhibited protease 1) and **RCR3** (Required for C*ladosporium fulvum* resistance 3) are two tomato PLCPs that accumulate in the extracellularly in the apoplast (Krüger *et al.*, 2002; Tian *et al.*, 2007). Both *PIP1* and *RCR3* map at the same genetic locus of tomato and are transcriptionally up-regulated during pathogen challenge (Krüger *et al.*, 2002; Tian *et al.*, 2007). Both proteases are inhibited by pathogen-derived inhibitors. PIP1 is inhibited by Epic2B, a cystatin-like protease inhibitor secreted during infection by the oomycete *Phytophthora infestans* (Tian *et al*., 2007). RCR3 is inhibited by Avr2, a secreted, cysteine-rich protein produced by the leaf mould fungus *Cladosporium fulvum* (Luderer *et al.*, 2002; Rooney *et al.*, 2005). The RCR3-Avr2 complex, and not RCR3 inhibition itself, triggers the hypersensitive response (HR) mediated by tomato resistance gene *Cf-2* (Rooney *et al.*, 2005). However, how Cf2 recognises the RCR3-Avr2 complex and the specificity of inhibition by Avr2 and Epic2B are not yet fully understood.

RD19 (*responsive to desiccation 19*) is a drought stress-induced PLCP (Koizumi *et al*., 1993). RD19 interacts with the effector protein PopP2 (Pseudomonas outer protein P2) from soil-born bacterial pathogen *Ralstonia solanacearum* and is required for resistance to *R. solanacearum* mediated by the RRS1-resistance gene (Bernoux *et al.*, 2008). A physical interaction between RRS1 and RD19 was not detected. However, RD19 re-localised from vacuole compartment to the nucleus upon PopP2 co-expression, suggesting that the nuclear complex is required for RRS1-mediated resistance (Bernoux *et al.*, 2008).

CatB (*Cathepsin B*) is another plant PLCP, named after the well-studied animal *Cathepsins* which play a role in defence in animals (Zavasnik-Bergant and Turk, 2006). Martinez *et al*. (2003) reported that the *CatB* gene in barley is ubiquitously expressed, in particular in developing organs and under circadian control. *CatB* expression increased upon cold shock, but was not altered by mechanical wounding (Martinez *et al*., 2003). In potato, transcript levels of *StCatB* are induced at early stages of infection

Phytophthora infestans on resistant plants (Avrova *et al.*, 2004). Induced transcription and CatB protease activity were also detected during the HR in *N. benthamiana* (Gilroy *et al.*, 2007). Importantly, *CatB* silencing suppresses the development of HR, suggesting that CatB acts in defence signalling (Gilroy *et al.*, 2007). Secretion of CatB into the apoplast was observed and this secretion triggers maturation and activation of the protease (Gilroy *et al.*, 2007).

1.4. Power of Activity-based protein profiling

Knowing when a protease is active is crucial since proteases occur as inactive precursors and are regulated by inhibitors. Activity-based protein profiling reveals the activity of proteases through a covalent labelling of proteases with biotinylated mechanism-based inhibitors, called probes (Greenbaum *et al.*, 2000). This method is widely applied in the medical field, but only starts to be used in plant science (Rooney *et al.*, 2005, Van der Hoorn, *et al.*, 2004). A first example of activity-based protein profiling in plants was by using DCG-04 (Van der Hoorn *et al.*, 2004). DCG-04 is a biotinylated derivative of E-64, an inhibitor of PLCPs, that irreversibly and covalently reacts with the catalytic cysteine (Greenbaum *et al.*, 2000). Using DCG-04 as a probe, six PLCPs were detected in Arabidopsis leaf extracts (Van der Hoorn, *et al.*, 2004). These include three previously studied proteases (RD21, AALP and XCP2) and three newly identified proteases, CatB1 (Cathepsin B-like protease 1), ALP2 (aleurain-like protease 2) and THI1 (TPE4-like protease) (Yamada *et al.*, 2001, Ahmed *et al.*, 2000, Zhao *et al.*, 2000).

1.5. RD21A

RD21 (At1g47128) is a PLCP which was initially found to be up-regulated in drought-stressed Arabidopsis and hence named responsive to desiccation-21 (Yamaguchi-Shinozaki *et al.*, 1992). Although transcript levels of *RD21* do not change upon treatment with heat, cold nor abscisic acid, *RD21* expression level increases upon water deficiency (drought stress) and high salt conditions (Koizumi *et al.*, 1993). RD21 contains an N-terminal signal peptide, a 20 kDa auto-inhibitory prodomain, a 33 kDa protease domain, a 2 kDa proline-rich domain and a 10 kDa granulin-like domain (Yamada *et al.*, 2001). Protease maturation occurs in steps, starting from 1) signal peptide release resulting in proRD21; 2) prodomain cleavage to form immature RD21 (iRD21); 3) granulin domain removal leading to mature RD21 (mRD21) (Figure 1.3). Studies with recombinant RD21, produced in insect cells, revealed that the prodomain cleavage is only triggered in the presence of plant extracts, indicating that the

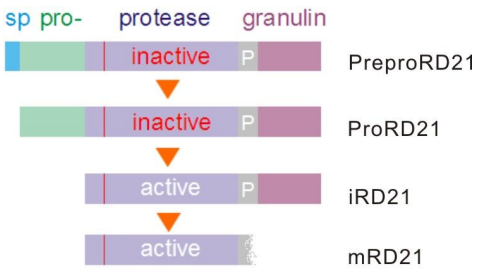

Fig. 1.3 RD21 maturation steps

RD21 maturation steps are shown. Preproprotein, precursor of RD21; proRD21, proprotein precursor of RD21; iRD21, intermediate RD21; mRD21, mature RD21; Sp, Signal peptide; Pro-, N-terminal pro-domain; Protease, protease domain; P, proline-rich domain; granulin, C-terminal granulin domain.

conversion of the proform into iRD21 is not autocatalytic (Yamada *et al.*, 2001). What triggers granulin domain removal is not understood, but both iRD21 and mRD21 are active as protease (Yamada *et al.*, 2001, Van der Hoorn *et al.*, 2004). Localisation studies indicate that iRD21 is transported from the Endoplasmic Reticulum (ER) with ER bodies, small cellular organelles released from ER, in vacuoles, where conversion into mRD21 occurs (Yamada *et al.*, 2001, Hayashi *et al.*, 2001, Carter *et al.*, 2004, Kikuchi *et al.*, 2008).

RD21-like proteases that carry a C-terminal granulin domain are found in many different plant species including tomato, maize, potato, rice, sweet potato, popla and radish (Schaffer and Fischer, 1990, Linthorst *et al.*, 1993, Tabaeizadeh *et al.*, 1995, Drake *et al.*, 1996, Yamada *et al.*, 2001B, Avrova *et al.*, 1999, Chen *et al.*, 2006, Garcia-Lorenzo *et al.*, 2006, Kikuchi *et al.*, 2008). For example, in tomato, C14 (also called as SENU2 or TDI-65) has been independently reported several times and *C14* transcript levels are induced by cold, drought and during leaf senescence (Schaffer and Fischer, 1990, Drake *et al.*, 1996, Tabaeizadeh *et al.*, 1995, Harrak *et al.*, 2001). During drought stress C14 is localized and accumulates upon in nuclei, chloroplasts and the cytoplasm (Tabaeizadeh *et al.*, 1995). The RD21-homologue of potato, CYP, is transcriptionally induced in early stages of *Phytophthora infestans* infection (Avrova *et al.*, 1999). A maize RD21 homologue has been reported and remains to be characterised (Yamada *et al.*, 2001B).

A unique feature of RD21 is its C-terminal granulin domain containing 14 cysteines. The granulins have a size of approximately 6 kDa in animals and 10 kDa in plants. Animal granulin proteins are encoded as tandem progranulins consisting of ~7 granulin domains, which can be released by processing (Bateman and Bennett, 1998). Plant granulins contain two extra cysteine residues which probably form an extra disulfide bridge within a putative extra β-hairpin (Tolkatchev *et al.*, 2001, Yamada *et al.*, 2001). Plants encode genes only a single granulin domain in a C-terminal fusion with PLCPs. Mammalian granulins are a family of growth factors that are expressed and activated upon wounding (Bateman and Bennett, 1998, Guerra *et al.*, 2007). A role

of granulins in plants is yet poorly understood.

1.6. Involvement of PLCPs in autophagy

Autophagy, meaning “eat oneself” in Greek, is an intracellular recycling system in eukaryotes, that recycles nutrients and degrade damaged or toxic components in the cell (Seay *et al.*, 2006). Autophagy is well characterised in yeast and orthologs of yeast autophagy genes seem to be involved in autophagy in plants as well (Bassham, 2007, Ketelaar *et al.*, 2004). In plants there are two major autophagic pathways, separated based on the capacity of cytoplasmic material taken up for destruction; microautophagy and macroautophagy. Macroautophagy engulfs regions of the cytoplasm into double-membrane autophagosomes which subsequently degrade the inner contents (Bassham *et al.*, 2006). While the digestion is taking place, autophagosomes fuse with the vacuole and release the autophagic body (inner compartment of autophagosome) into the lumen of the vacuole. In contrast, microautophagy is formed from the vacuole membrane where small vesicles containing cytoplasmis materials are released into the vacuolar lumen for degradation (Bassham *et al.*, 2006). Autophagosomes can also fuse with small lysosomes or endosomes to form the autolysosome (Bassham, 2007). The contents of the autolysosome is degraded before it fuses with the vacuole.

Several autophagy (ATG) genes are required for autophagy and these can be grouped into five classes according to their functions; protein kinases, which are involved in the initiation or regulation of autophagosome; the phosphatidylinositol 3-kinase complex; two ubiquitin-like conjugation systems and formation of ATG9 complex (Table. 1.1) (Bassham, 2007, Seay *et al.*, 2006). Knock-out of *ATG* genes in plants often display accelerated leaf senescence and defects in nutrient remobilization during sugar and nitrogen starvation (Bassham, 2007). Autophagy in plants is also involved in degradation of oxidised proteins and disposal of protein aggregates (Xiong *et al.*, 2007, Bassham, 2007). Moreover, like in animals, autophagy contributes to innate immune responses since silencing of the *ATG6*/*Beclin1* homologue in *N. benthamiana* causes uncontrolled programmed cell death (PCD) upon infection with avirulent tobacco mosaic virus (TMV) (Liu *et al.*, 2005).

ATG8 is a ubiquitin-like proteins essential for autophagy (Ketelaar *et al.*, 2004). ATG8 modification requires two proteins, ATG3 and ATG4. ATG4 is cysteine protease (Clan CA, family C54) that exposes the C-terminal Gly of ATG8 (Thompson and Vierstra, 2005, Yoshimoto *et al.*, 2004). ATG3 is an E2-like ligase that ligate ubiquitin-like ATG8 after the C-terminal modification (Thompson and Vierstra, 2005,

Table 1.1 Proteins involved in autophagy (Adapted from Bassham, 2007)

Function groups	Proteins	Putative function
Regulation	TOR, ATG1, 13, 11, 19	Initiation of autophagy
PI-3 kinase complex	ATG6, VPS15, VPS34	Autophagosome formation
Ubiquitin-like conjugation	ATG5, 7, 10, 12, 16	Conjugation of ATG12 and ATG5
	ATG3, 4, 7, 8	Conjugation of ATG8 to phosphatidylethanolamine
ATG9 complex & localization	ATG9, 2, 18	Membrane recruitment to autophagosome
SNARE	VTI12	Fusion of autophagosomes with the vacuole

Tanida *et al*., 2006). Interestingly, plant cells incubated with E-64 or concanamycin A result in the accumulation of autolysosomes in the cytoplasm during sugar starvation (Bassham, 2007, Moriyasu *et al*., 2003, Inoue *et al*., 2006). Furthermore, E-64 inhibition of ATG8 modification, without inhibiting ATG4, has been reported (Alvarez *et al*., 2008). Although, E-64 is a specific inhibitor of PLCPs, a contribution of PLCPs to autophagy has not been reported so far.

1.7. Towards functional analysis of RD21

Previously, challenge of Arabidopsis cell suspension cultures with *Pst* revealed that *Pst* infection leads to differential protease activities of RD21 (Renier van der Hoorn unpublished data, done in John Iness Centre Norwich, UK). At 24 hours post inoculation (hpi), RD21 activity was induced during infection with avirulent *Pst DC3000 AvrRpm1* and suppressed during infection with virulent *Pst DC3000* (Van der Hoorn, unpublished). Strikingly, RD21 protein levels remain similar. This post-translational suppression of RD21 activity indicates that RD21 has a role in plant-microbe interactions and that there is an RD21 inhibitor secreted by *Pst*. Indeed, later during the cause of this PhD study, it was found that *Pst* secrets an RD21-inhibiting protein (RIP1) (Kaschani and Van der Hoorn, unpublished). Also *Phytophthora infestans* secrete inhibitors called EPIC protein preferentially target C14 (Shabab and Van der Hoorn, unpublished). These data prompted us to test if RD21A is involved in defence.

2 Results

2.1 Phenotyping Arabidopsis PLCP mutants

2.1.1 PLCP mutant collection

The Arabidopsis genome encodes for ~30 PLCPs which belong to eight subfamily according to the phylogenetic analysis of plant PLCPs (Figure 1.2, Beers *et al*. 2004). Hereafter, the above described RD21 is called as RD21A.

To study the role of PLCPs in plants, a collection of mutants was generated from publicly available SALK or GABI collections. T-DNA insertions were confirmed using gene-specific primers and homozygous mutant plants were selected and analysed in subsequent generations. The mutants are listed in Table 2.1A. Double mutants of homologous gene pairs, including *rd21A* x *rd21B, rd21B* x *rd21D, rd21A* x *rd21D*, *rd21A* x *rd21B* x *rd21D*, *aalp* x *alp2*, *xcp2* x *xcp1* and *catB1* x *catB2*, were generated (Table2.1B). When activity-based DCG-04 profiling was applied to leaf extracts of this mutant collection, signals were absent at 30 kDa and 25 kDa in *rd21A* and *aalp* mutants, respectively (Figure 2.1.1). This is consistent with the identified proteases described previously (Van der Hoorn *et al.* 2004), confirming that signals detected at 30 kDa and 25 kDa in DCG-04 profiles are predominantly caused by these two proteases. None of the stable homozygous mutants displayed an obvious phenotype when grown under normal greenhouse conditions.

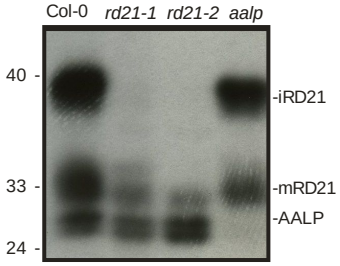

Figure 2.1.1. Activity-based DCG-04 profiling of *rd21* and *aalp* mutants. DCG-04 protease activity profiles of leaf extract of *rd21-1*, *rd21-2* and *aalp* mutants. Molecular weight (in kDa) are indicated on the left of the image. Biotinylated proteins were detected with streptavidin-HRP.

2.1.2 Pathogen assays on *rd21A* knock-out lines

To test if *RD21A* plays a role in plant-microbe interactions, two independent *rd21A* mutant lines (*rd21A-1* and *rd21A-2*) were subjected to pathogen assays. Mutant lines were challenged with *Pst DC3000* and the bacterial growth was monitored up to 3 days post inoculation (dpi) by colony counting. *rd21A* lines did not show an increased susceptibility when compared to wild type (Figure 2.1.2A). Similarly, infection with avirulent strains expressing AvrRpm1 (Figure 2.1.2B), AvrRpt2 or AvrRps4 (data not shown) did not display altered infection phenotypes. This indicates that growth of both virulent and avirulent *Pst* is not affected in *rd21A* mutants.

Table 2.1A Arabidopsis PLCP knock-out collection

Gene	Atg code	Source	Mutant
RD21A	At1g47128	SALK_90550	*rd21A-1*
		SALK_65256	*rd21A-2*
		GABI_401H08	*rd21A-4*
		GABI_792G08	*rd21A-3*
RD21B	At5g43060	SAIL_781H05	*rd21B-1*
RD21D	At1g09850	SALK_138483	*rd21D-1*
XCP1	At4g35350	SALK_84789	*xcp1-1*
XCP2	At1g20850	SALK_10938	*xcp2-1*
		SALK_57921	*xcp2-2*
SAG12	At5g45890	SALK_124030	*sag12.1*
RD19A	At4g39090	SALK_31088	*rd19A-1*
AALP	At5g60360	SALK_75550	*aalp-1*
AALP2	At3g45310	SALK_88620	*aalp2-1*
CatB1	At4g01610	SALK_19630	*catB1-1*
CatB2	At1g02300	SALK_63455	*catB2-1*
		SALK_110946	*catB2-2*
		SALK_151526	*catB2-3*
CatB3	At1g02305	SALK_89030	*catB3-1*

Table 2.1B Double and triple PLCP mutants

Transgenics	Atg codes	Gene	Source
rd21AB	At1g47128	*RD21A*	SALK_90550
	At5g43060	*RD21B*	SAIL_781H05
rd21ABD	At1g47128	*RD21A*	SALK_90550
	At5g43060	*RD21B*	SAIL_781H05
	At1g09850	*RD21D*	SALK_138483
xcp1xcp2	At4g35350	*XCP1*	SALK_84789
	At1g20850	*XCP2*	SALK_10938
aalp1alp2	At5g60360	*AALP*	SALK_75550
	At3g45310	*ALP2*	SALK_88620
catB1catB3	At4g01610	*CatB1*	SALK_19630
	At1g02305	*CatB3*	SALK_89030
rd21Aaalp	At1g47128	*RD21A*	SALK_90550
	At5g60360	*AALP*	SALK_75550

To test the susceptibility to other biotrophic pathogens, *rd21A* mutant lines were challenged with *Hyaloperonospora parasitica*. *rd21A-1* and *rd21A-2* lines did not show a significant increase in the number of spores at 7dpi upon inoculation with *H. parasitica* isolate *Noco2* (Figure 2.1.2C). Moreover, infection of *rd21A* lines with *H. parasitica* isolate *Emwa1* did not change the number of spores compared to wild type plants at 7dpi (Figure 2.1.2D). *rd21A* mutant lines were also challenged with two necrotrophic pathogens, *Alternaria brassicicola* and *Botrytis cinerea*, as well as the semi-biotrophic pathogen *Colletotricum higginsianum*. Spread of the pathogen upon droplet inoculation was scored at 5dpi. In case of *C. higginsianum* and *A. brassicicola*, *rd21A* mutants did not show an altered susceptibility (Figure 2.1.2E,F). In contrast, *rd21A* mutants were significantly more susceptible to *B. cinerea* inoculation, with 15 to 25% increased infection rates (Figure 2.1.2G). This shows that *rd21A* mutants are more susceptible to the necrotrophic pathogen *B. cinerea*, but not to other pathogens tested.

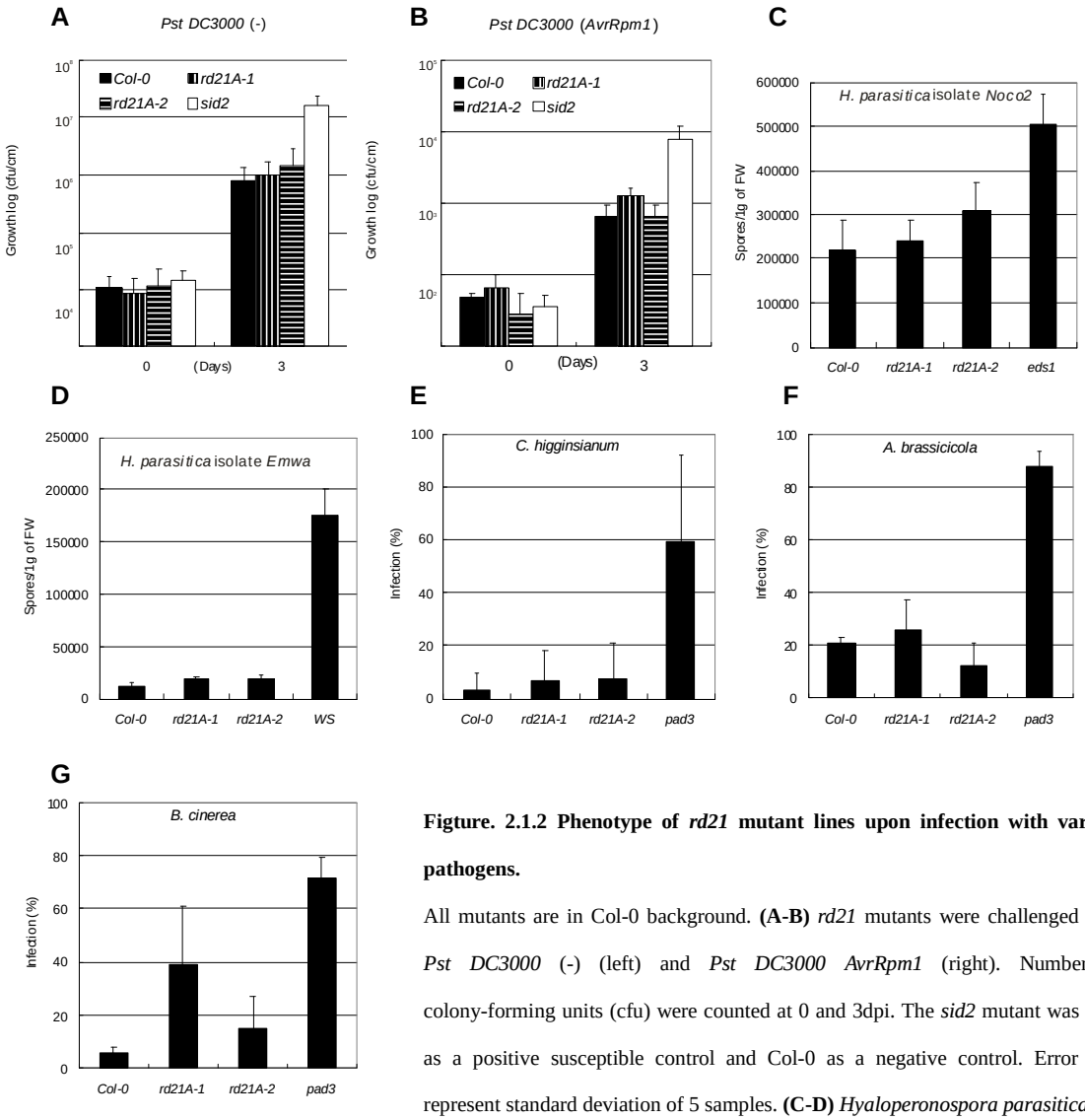

Figture. 2.1.2 Phenotype of *rd21* mutant lines upon infection with various pathogens.

All mutants are in Col-0 background. **(A-B)** *rd21* mutants were challenged with *Pst DC3000* (-) (left) and *Pst DC3000 AvrRpm1* (right). Number of colony-forming units (cfu) were counted at 0 and 3dpi. The *sid2* mutant was used as a positive susceptible control and Col-0 as a negative control. Error bars represent standard deviation of 5 samples. **(C-D)** *Hyaloperonospora parasitica, Noco2* and *Emwa,* assays on *rd21* knock-out lines. Spore counts were performed at 7dpi. Error bars represent the standard deviation of 3 samples. **(E)** *Colletotricum higginsianum* assay on *rd21* knock-out lines. Plants were inoculated with droplets containing *C. higginsianum* spores. Outgrowth was monitored at 5dpi. *pad3* mutant was used as a positive control and Col-0 as a negative control. Error bars represent standard deviation of 30 samples. **(F)** *Alternaria brassicicola* assay on *rd21* knockout lines. Plants were inoculated with droplets containing *A. brassicicola* spores. Outgrowth was monitored at 5dpi. Error bars represent the standard deviation of 30 samples. **(G)** *Botrytis cinerea* assays on *rd21* knockout lines. Plants were inoculated with droplets containing *B. cinerea* spores. Spore counts were performed at 7dpi. *pad3* mutant was used as a positive control. Error bars represent the standard deviation of 10 samples.

2.1.4 RD21A over-expression

RD21A protein was over-expressed *in planta* to investigate if it causes a phenotype. Full length *RD21A* was cloned into a plasmid behind the *CaMV 35S* promoter and transformed into *Agrobacterium* (Van der Hoorn, unpublished). Transient over-expression of *35S::RD21A* by Agrobacterium infiltration into *N. benthamiana*

resulted in high RD21A protein and activity levels, demonstrating that the construct is functional (data not shown). However, no phenotype was observed upon infiltration despite the fact that an active protease is over-expressed. The same construct was stabely transformed into the ecotype Arabidopsis (Col) generating RD21A over-expressing plants. Lines were selected that showed enhanced RD21A protein and activity levels (data not shown). These lines did not display a phenotype under standard greenhouse conditions. Pathogen assays with *Pst* (*DC3000*), *H. parasitica* (*Noco2*), *C. higginsianum, A. brassicicola* or *B. cinerea did* not show any phenotype when compared to wild-type Arabidopsis (data not shown).

2.1.5 RD21 triple knock-out line

There are four genes encoding granulin containing proteases in Arabidopsis, named RD21A, RD21B (At5g43060), RD21C (At3g19390) and RD21D (At1g09850) (Figure 1.2). Microarray data indicate that these proteases overlap in their expression patterns in leaves and that only RD21C is distinctively expressed in roots (Appendix. 1) (*Zimmermann et al*., 2004, Genevestigator: https://www.genevestigator.ethz.ch). It was hypothesised that the lack of phenotype during *Pseudomonas* infection was due to redundancy with other granulated proteases. We, therefore, aimed at generating a quadruple knock-out line lacking all granulated proteases to investigate the role of these enzymes. Knock-out lines *rd21B* and *rd21D* were obtained from SAIL and SALK line collections, respectively, and were confirmed by genomic PCR. T-DNA insertion lines in *RD21C* were not available. We screened the Koncz T-DNA insertion collection (Rios *et al*., 2002). Two candidates were found in the screening but the T-DNA insertions in both cases were detected more than 50 bp after the end of open reading frame (data not shown).

All possible double knock-out lines and the triple knock-out lines, *rd21ABD*, were generated by crossing (Table. 2.1B). There was no phenotype observed under normal greenhouse conditions. To test if the absence of three granulated proteases alters pathogen susceptibility, the triple *rd21ABD* knock-out line was challenged with various pathogens. The *rd21ABD* triple knock-out line was not more susceptible to *Pst* (*DC3000*), *H. parasitica* (both *Noco2* and *Emwa1*), *C. higginsianum* and *A. brassicicola* compared to wild-type Arabidopsis (Figure 2.1.3A-E). In the case of *B. cinerea* inoculation, however, there was approximately 30% increase of fungal infection when compared to wild-type (Figure 2.1.3F-G). This indicates that *rd21ABD* show the increased susceptible phenotype to *B. cinerea*, but not other pathogens tested.

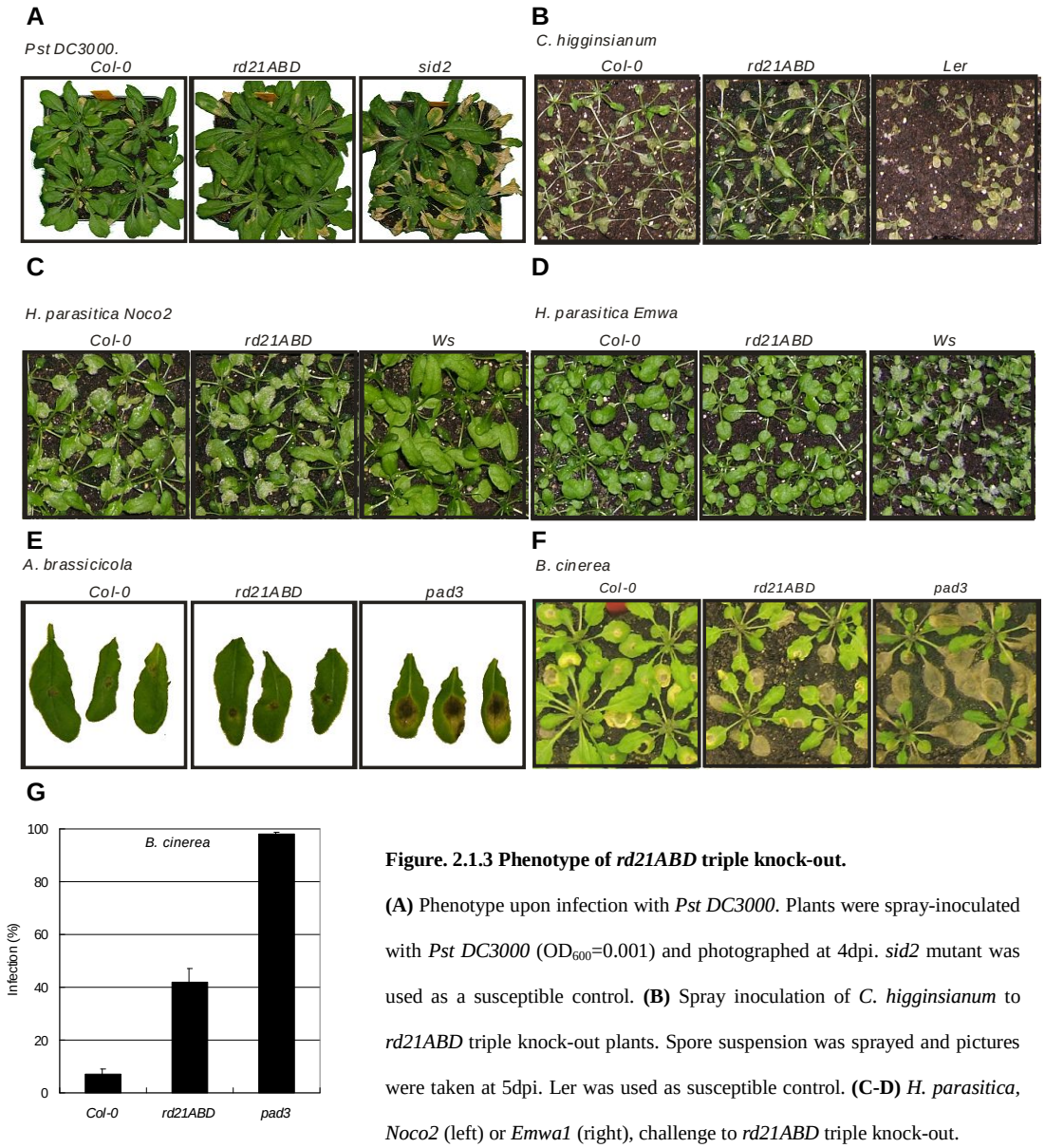

Figure. 2.1.3 Phenotype of *rd21ABD* triple knock-out.

(A) Phenotype upon infection with *Pst DC3000*. Plants were spray-inoculated with *Pst DC3000* (OD_{600}=0.001) and photographed at 4dpi. *sid2* mutant was used as a susceptible control. **(B)** Spray inoculation of *C. higginsianum* to *rd21ABD* triple knock-out plants. Spore suspension was sprayed and pictures were taken at 5dpi. Ler was used as susceptible control. **(C-D)** *H. parasitica*, *Noco2* (left) or *Emwa1* (right), challenge to *rd21ABD* triple knock-out. Spore suspension was sprayed and pictures were taken at 7dpi. In both cases, ecotype *Ws* was used as a control. **(E)** Droplet inoculation of *A. brassicicola* to *rd21ABD* triple knock-out. Spore suspension was used for droplet inoculation. At 5dpi inoculated leaves were detached and photographed. *pad3* was used as a positive susceptible control. **(F)** Droplet inoculation of *B. cinerea* on *rd21ABD* triple knock-out. A droplet of spore suspension was inoculated on a leaf. Pictures were taken at 5dpi. **(G)** Percentage of *B. cinerea* outgrowth in *rd21ABD* was determined. Error bars represent the standard deviation of 100 samples. *pad3* was used as a susceptible control.

2.2. Do PLCPs play a role in defence in tomato?

The following section was a part of Shabab *et al.* 2008 is shown below. This was accomplished together with R. A. L. Van der Hoorn.

2.2.1. Transcript level of some PLCPs up-regulated by BTH treatment

BTH is an analogue of salicylic acid (SA) and triggers the salicylic acid dependent defence pathway in plants (Achuo *et al.*, 2004). To investigate if any of the PLCPs are also regulated by SA, transcriptional changes of genes encoding PLCPs were studied after BTH treatment. As shown in figure 2.2.1A, transcript levels of two *PR* (*Pathogenesis Related*) genes, *PR1* and *PR4*, significantly increased at 5 days after BTH treatment. Accumulation of transcripts occurred also for genes encoding *PIP1* and *RCR3* (Figure2.2.1A). The other PLCPs tested (*C14*, *Cyp3*, *Alp*, *CatB1* and *CatB2*) were not induced by BTH treatment to high levels. Quantitative RT-PCR revealed that there was an eight-fold induction of both *Pip1* and *RCR3* upon BTH treatment, while there were only minor or no changes in the other genes tested (Figure 2.2.1B).

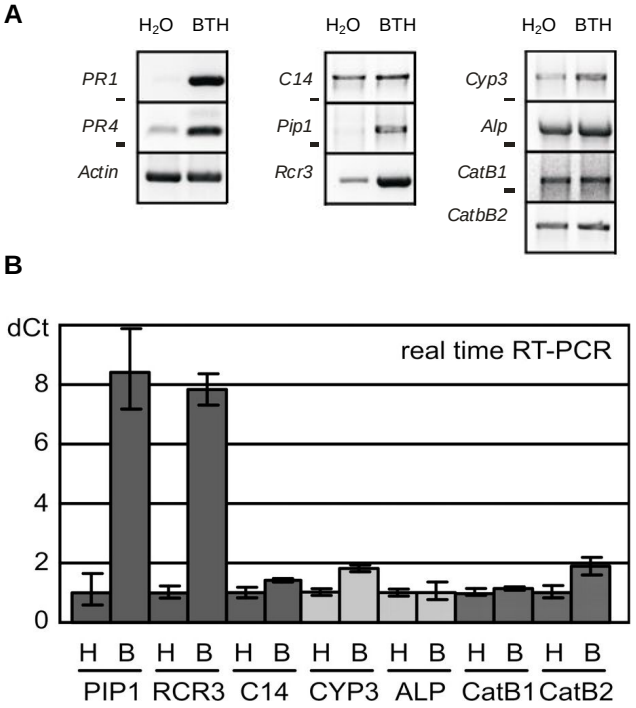

Figure 2.2.1 Induction of transcript levels of tomato PLCPs upon BTH treatment.

Tomato leaves were harvested at 5 days after water or BTH treatment.

(A) RT-PCR was performed using gene-specific primers. Actin was used as a control.

(B) Quantitative real-time RT-PCR was performed using gene-specific primers. The difference in threshold cycles (dCt) between the protease transcript and ubiquitin transcripts was calculated from three independent samples. Error bars represent SD. A representative of five independent biological experiments is shown.

2.2.2. Some PLCPs are under diversifying selection

Defence-related enzymes might be involved in antagonistic interactions with pathogens-derived substrates or inhibitors (Misas-Villamil and Van der Hoorn, 2008).

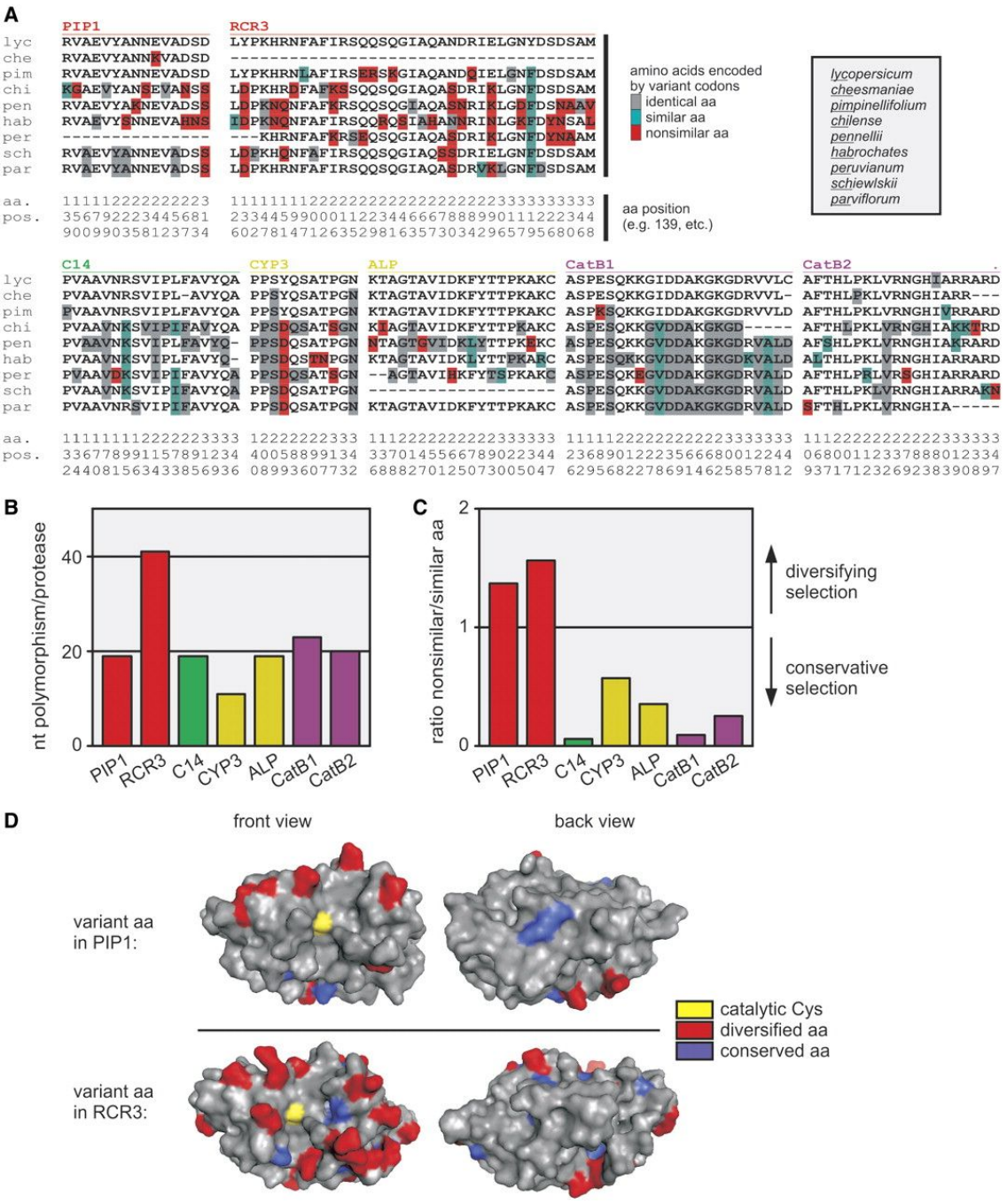

Figure 2.2.2 Sequence analyses of PLPCs from tomato relatives.

(A) Summary of amino acids encoded by variant codons in the protease domains of C14, PIP1, RCR3, CYP3, ALP, CatB1, and CatB2 alleles sequenced from various wild tomato relatives (indicated top right). Amino acids encoded by the variant codons are summarized by leaving out the amino acids of nonvariant codons from the protein alignment. Amino acids encoded by codons different from the *S. lycopersicum* (*lyc*) allele are indicated with gray, blue, and red residues if they are identical, similar, or nonsimilar, respectively, compared with the *lyc* sequence. Dashes indicate missing sequence information. RCR3 of *S. cheesmanniae* is not shown since it contained a premature stop codon and could be amplified from genomic DNA and not from cDNA.

(B) Number of single nucleotide (nt) polymorphisms per protease. **(C)** Ratio of nonsimilar/similar amino acid (aa) substitutions calculated from (A). PIP1 and RCR3 are under diversifying selection; the other proteases are under conservative selection.

(D) Position of variant residues in structural models of PIP1 and RCR3. Positions with nonsimilar variance and similar variance are indicated in red and blue, respectively.

To investigate if tomato PLCPs are under evolutional selection to be diverse, we sequenced the region encoding the protease domain of eight wild tomato relatives: *S. cheesmanniae*, *S. pimpinellifolium*, *S. chilense*, *S. pennellii*, *S. habrochates* (*hirsutum*), *S. peruvianum*, *S. schiewlskii*, and *S. parviflorum*. Sequences of theses alleles were validated and found to be 98% identical to the reported tomato sequences. Amino acids encoded by the polymorphic codons of all the protease domains are shown in Figure 2.2.A. The protease-coding part of each gene contains about 20 variant nucleotides, except for *RCR3*, which has 41 variant nucleotides (Figure 2.2.2B). Some of the variant nucleotides are shared among different species, indicating that part of the variation predates speciation (Figure 2.2.2A). Most of the polymorphic nucleotides, however, are allele-specific. The consequence of these variant residues at amino acid level is striking. Variant codons hardly change the encoded amino acids in C14, CYP3, ALP, CatB1, and CatB2 (Figure 2.2.2A, bottom, white and gray residues). By contrast, nearly all variant codons of *PIP1* and *RCR3* cause nonsimilar amino acid substitutions (Figure 2.2.2A, bottom, red residues). The ratio between nonsimilar and similar amino acids indicates that C14, CYP3, ALP, CatB1, and CatB2 are under conservative selection, whereas PIP1 and RCR3 are under diversifying selection (Figure 2.2.2C). Taken together, these observations demonstrate that PIP1 and RCR3 are under diversifying selection, possibly to adapt to diversifying substrates or inhibitors, whereas the other proteases are under conservative selection.

2.3 Analysis of *NbRd21* silencing

2.3.1. Virus-induced gene silencing of RD21 in *N. benthamiana*

When the protein sequence of the granulin domain of Arabidopsis RD21A was blasted at TIGR using tBLASTn (http://plantta.tigr.org/), there were two highly homologues cDNA sequences found in *N. benthamiana*, *NbRd21-I* (TC7740/ CN743238) and *NbRd21-II* (EST748747/CK286025). *NbRd21-I* encodes a full length protease whereas *NbRd21-II* is incomplete at the 5' end and only encodes part of the protease domain followed by granulin domain. There is a 362 bp region 81% homology in both *NbRD21-I* and *NbRd21-II* on nucleotide level (Figure 2.3.1A, coloured in yellow). The amino acid sequence *NbRd21-I* is 42% identical and 58% similar to *C14* of tomato and 43% identical and 59% similar to *RD21B* in Arabidopsis. Three regions of about 300 bp were selected from *NbRd21-I* (α, β and γ) and one from *NbRd21-II* to generate TRV-based silencing constructs. *NbAlp* (TC7311) was taken as a protease control for silencing. The *NbAlp* encodes a protease that is 78% identical to Arabidopsis AALP.

TRV-based virus-induced silencing was initiated by infiltrating Agrobacterium cultures carrying the binary *TRV* constructs into four week-old *N. benthamiana* plants. *TRV* constructs containing fragments of *GFP* or *NbAlp* were used as controls for silencing. Semi-quantitative RT-PCR on RNA isolated from systemic leaves at 21 dpi confirmed selective silencing (Figure 2.3.1B.). Importantly all *NbRd21* silencing constructs suppress transcript levels of both *NbRd21* genes (Figure 2.3.1B.). Thus, all *NbRd21-I* silencing constructs co-silence *NbRd21-II* and *vice-versa*. Silencing of *NbRd21* was not observed in plants inoculated with *TRV::Alp* or *TRV::GFP*, but *NbAlp* transcript levels are dramatically reduced in *TRV::Alp* plants (Figure 2.3.1B.). Quantitative real-time RT-PCR showed that in *TRV::NbRd21-I* plants the transcript levels of *NbRd21-I* and *NbRd21-II* are reduced by 80% and 65%, respectively (Figure 2.3.1C.). In contrast, in *TRV::NbRd21-II* plants, transcript levels of *NbRd21-I* and *NbRd21-II* are reduced by 40 and 85%, respectively (Figure 2.3.1C.). This implies that, although transcript levels of both genes are suppressed, the genes corresponding to the silencing construct are more severely silenced. No difference in the silencing level was observed between all three independent *NbRd21-I* silencing constructs.

To study the effect of silencing on protease activity levels, activity-based profiling using DCG-04 was performed on protein extracts from systemic leaves of silenced plants. Activity profiles of *TRV::GFP* plants show bands at 40, 33, 30 and 28 kDa (Figure 2.3.1D.). In Arabidopsis leaf extract, signals of 40 and 33 kDa are caused

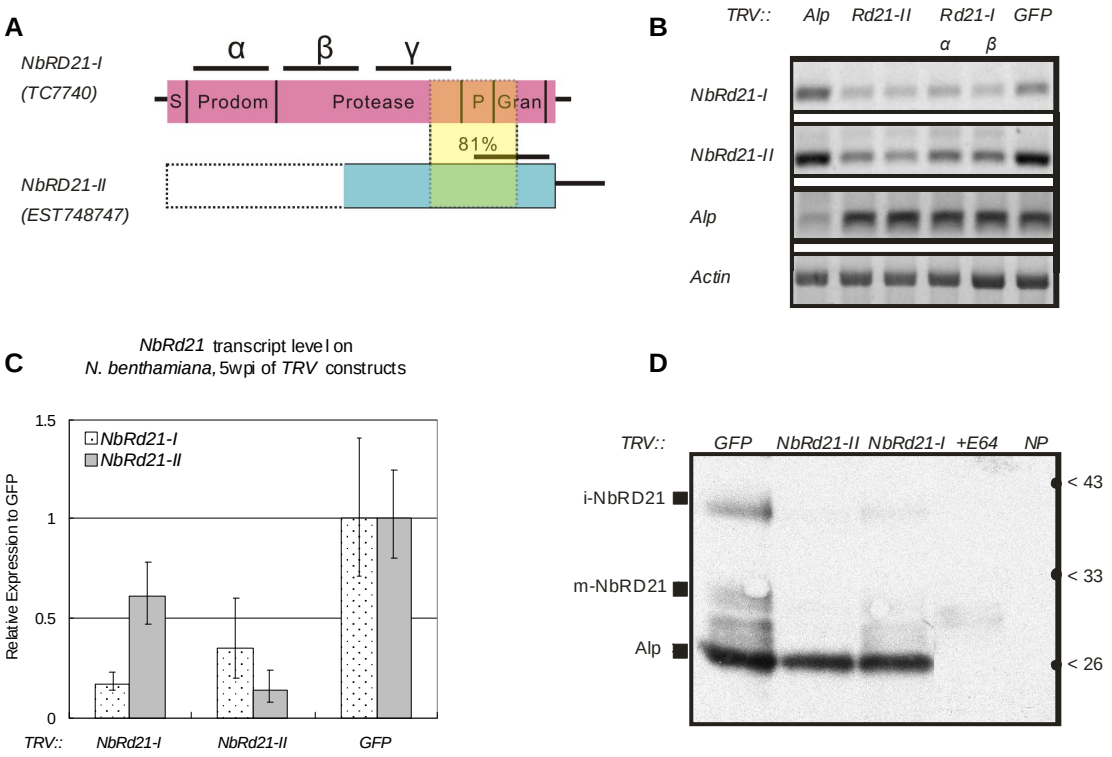

Figure 2.3.1 ***NbRd21*** **silencing constructs co-silence both** ***NbRd21-II*** **and** ***NbRd21-II***

A) Fragments used for silencing constructs. Two cDNA sequences encoding RD21-like proteases of *N. benthamiana* are available at the TIGR database. The sequence of *NbRd21-II* is incomplete (dashed lines). Lines above the bars indicate the regions used for silencing constructs for virus-induced gene silencing (VIGS). The region coloured in yellow indicates 81% nucleotide identity. S, Signal peptide; Prodom, N-terminal pro-domain; Protease, protease domain; P, proline-rich domain; Gran, C-terminal granulin domain. B) Transcript levels in systemic leaves of *N. benthamiana* plants inoculated with various silencing constructs at 28 dpi. Gene-specific primers were used for semi-quantitative RT-PCR. Actin was used as a control. C) Transcript levels in systemic leaves of *N. benthamiana* plants inoculated with *NbRd21* silencing constructs at 28 dpi. Gene-specific primers were used for Realtime RT-PCR. Transcript levels were normalised to that of GFP silenced plants. D) DCG-04 activity profiling on extracts of systemic leaves of silenced plants at 28 dpi. NP, no probe control; +E-64, excess of E-64 to compete for DCG-04 labelling.

by the immature (i) and mature (m) isoform of RD21A, respectively, whereas the 28 kDa signal represents AALP (Van der Hoorn *et al.*, 2004). In both *TRV::NbRd21-I* and *TRV::NbRd21-II* plants, both 40 and 33 kDa signals were reduced whereas the 28 kDa signal is as intense compared to *TRV::GFP* plants (Figure 2.3.1D.) indicating that *NbRd21* silencing suppresses NbRD21 activity in systemic leaves.

2.3.2. *TRV::NbRd21* triggers cell death

Importantly, all *TRV::NbRd21* plants showed retarded growth at 14 days after infiltration (Figure 2.3.2A.). By 28 dpi there was a clear growth retardation of

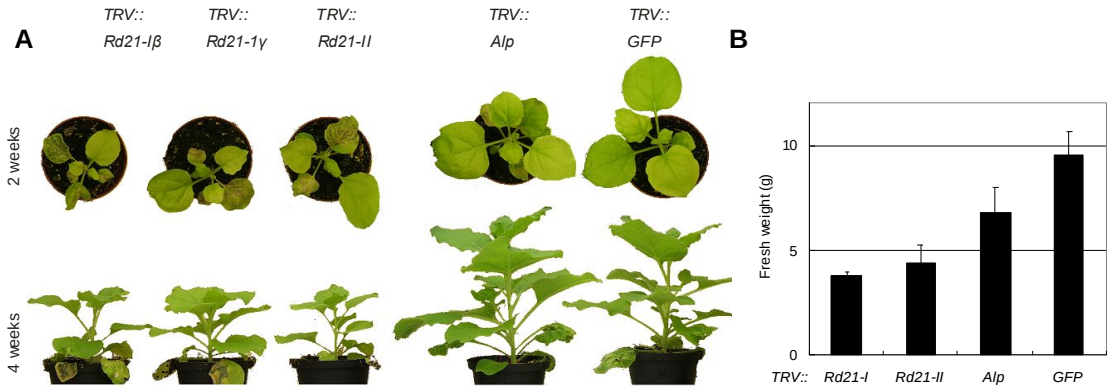

Figure 2.3.2 Phenotype of *N. benthamiana* upon virus induced gene silencing of *NbRd21*

(A) 4-week old *N. benthamiana* plants were infiltrated with *Agrobacterium* carrying binary TRV constructs, and photographed at 2 and 4 weeks after infiltration. *TRV::Alp* (*Aleurain-like protease*) and *TRV::GFP* were used as controls. **(B)** Fresh weight of plants at 5 weeks after inoculation with TRV constructs. Results shown represent the average weight of three plants. Error bars represent SD. A representative of three biological replicates is shown.

TRV::NbRd21 plants in contrast to *TRV::Alp* or *TRV::GFP* plants, both in size and weight (Figure 2.3.2B.). When the plants were more carefully investigated, *TRV::NbRd21* plants showed cell death on both the infiltrated leaf and the leaf above the infiltrated leaf.

To monitor cell death development in more detail, TRV constructs were infiltrated into mature leaves of *N. benthamiana*. No difference was observed between *TRV::GFP* and *TRV::NbRd21* infiltrated leaves during the first two days. At 3 dpi, however, cell death started to appear in and around the *TRV::NbRd21* infiltrated region (Figure 2.3.3A.). This was followed by the formation of a ring-shaped cell death at 4 to 5 dpi surrounding the infiltrated zone (Figure 2.3.3A.). The cell death eventually spread out through the leaf as well as inside the infiltrated zone by 9 dpi (Figure 2.3.3A.). In many cases, spreading of cell death reached the vein of the leaf in seven days and migrates to the stem and upper leaves within 14 days.

In order to characterize how the cell death spreads, *TRV::NbRd21*-infiltrated leaves were stained with trypan blue that stain dead cells blue. This assay revealed that spots of cell death develop in the infiltrated region at 3 dpi (Figure 2.3.3B.). These spots of cell death were larger on the edge of the infiltrated zone than inside the infiltrated area (Figure 2.3.3B.). Formation of the ring-shaped cell death occurs around the *TRV::NbRd21* infiltrated area at 5 dpi which leads to the cell death spreads (Figure 2.3.3B.). No cell death was detected in *TRV::GFP* infiltrated leaves at any of the

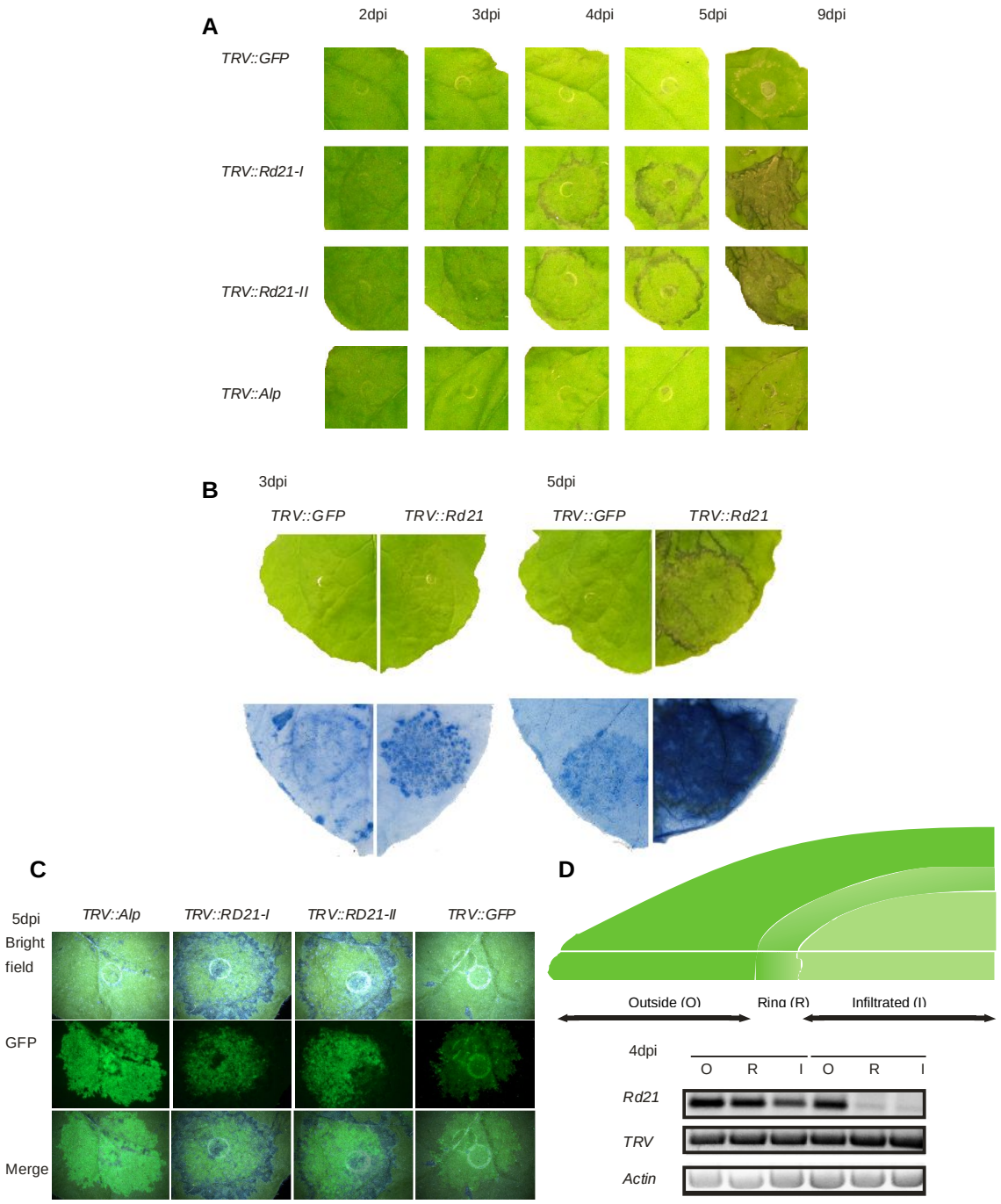

Figure 2.3.3 Cell death develops around the infiltrated region of *TRV::NbRd21*

(A) Infiltration of TRV constructs into mature *N. benthamiana* leaves. Images were taken at different days post infiltration (dpi). **(B)** Trypan blue staining of TRV infiltrated leaves. Infiltrated leaves (top) were stained by Trypan blue (bottom); dead cells are stained blue. **(C)** Cell death develops around the infiltrated region. TRV constructs were co-infiltrated with a GFP construct. Pictures were taken at 5dpi with a fluorescence microscope under bright field and under GFP filter. **(D)** Transcript level of in and around the infiltrated area. As the schematic diagram (top) shows, leaves infiltrated with *TRV::NbRD21* or *TRV::GFP* were sampled in three different sections; Infiltrated (I), Ring around the infiltrated region (R) or Outside (O). RT-PCR was performed to detect transcript levels of *NbRd21*, TRV and actin (control).

analysed time points.

To specify the region where the cell death ring develops, *TRV::NbRd21* constructs were co-infiltrated with *Agrobacterium* containing a 35S::GFP binary construct. This method enables us to visualize the infiltrated zone by GFP fluorescence. At 5 dpi the cell death ring was formed precisely along the edge of the fluorescent area (Figure 2.3.3C.). This demonstrates that cell death occurs in the *Agrobacterium*-free region, surrounding the infiltrated zone.

To detect transcript levels in and around the infiltrated area, three samples were taken from *Agrobacterium* infiltrated leaves; the infiltrated region (I), the edge of infiltrated zone (R, where cell death "ring" would occur at 5dpi) and further outside the infiltrated area (O) (Figure 2.3.3D.). Sample collection took place at 3dpi before the ring of cell death appears. The three portions of leaves were analysed by semi-quantitative RT-PCR. *TRV::NbRd21* infiltration suppresses *NbRd21* transcript levels already at 3dpi in the infiltrated region and, interestingly, in the ring as well (Figure 2.3.3D.). In contrast, RNA levels of the TRV is high in all regions at 3dpi, implying that TRV movement is a fast process that causes TRV RNA accumulation outside the infiltrated area. Taken together these results indicate that cell death in the ring is preceded by strong *NbRd21* silencing

2.3.3. What is the trigger of cell death in *NbRd21* silencing?

Since the transient expression system used to introduce *TRV::NbRd21* inevitably introduces also *Agrobacterium*, it was not clear if *Agrobacterium* contributes to the cell death phenotype. To rule out the potential *Agrobacterium* involvement to cell death, sap containing virions isolated from *TRV::NbRd21* and *TRV::GFP* plants at four weeks after inoculation (Figure 2.3.4. left). When sap containing *TRV::NbRd21* virions were injected into leaves of new *N. benthamiana* plants, the inoculation resulted in spreading cell death at 5 dpi (Figure 2.3.4. right). Sap containing *TRV::GFP* virions or leaf extract from non-infected plants did not trigger cell death. Additionally, no *Agrobacterium* was detected when sap was plated on kanamycin and rifampicin containing plates, implying there was no *Agrobacterium* in the sap (data not shown). This demonstrates that Agrobacterium is not required for *TRV::NbRd21* induced cell death.

In order to uncouple *NbRd21* silencing from TRV, RNAi hairpin (hp) constructs, *hpNbRd21,* were generated using the same fragments from *NbRd21* used to generate the *TRV::NbRd21* constructs. RT-PCR at 5 dpi of *hpNbRd21*-infiltrated leaves showed reduced *NbRd21* transcript levels in the infiltrated region (data not shown).

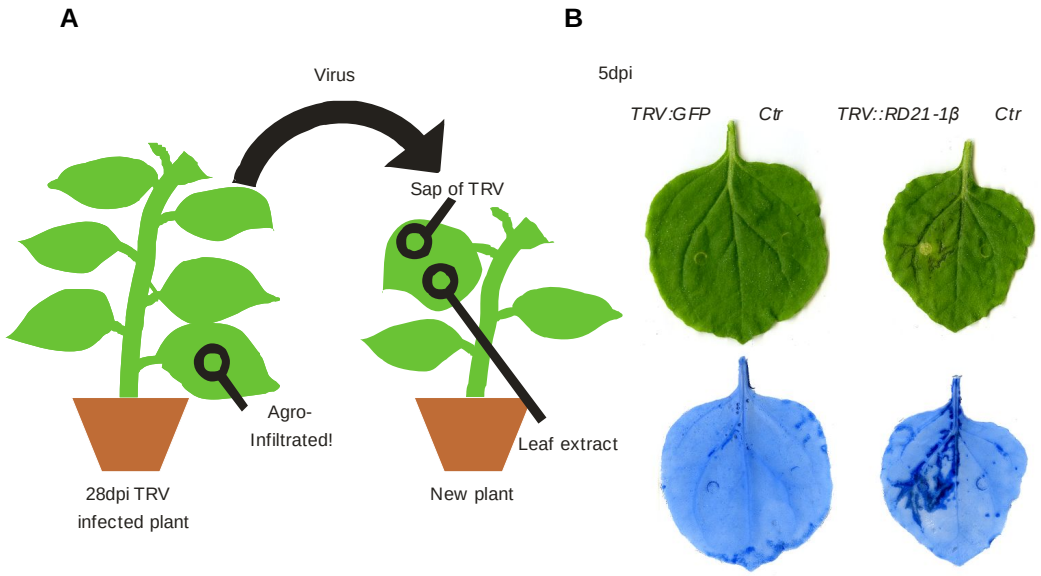

Figure 2.3.4 Cell death is induced by *TRV::NbRd21* in the absence of Agrobacterium

(A) Infiltration of TRV virus to mature leaves. Virions, isolated from TRV-infected plants at 4 weeks after infiltration, were infiltrated to non-silenced mature leaves (left half of leaves). **(B)** Images were taken (top) and leaves were stained by Trypan blue (bottom). Control (Ctr) leaf extract was isolated from non-infected plants and infiltrated in the right half of the leaves

However, despite *hpNbRd21* silencing, no cell death or other phenotypic changes were observed (data not shown). This implies that TRV is needed as an inducer of cell death. Therefore, *hpNbRd21* was co-infiltrated with *TRV::GFP* to reconstitute the cell death phenotype. However, co-infiltration of both *TRV* and *hpNbRd21* did not result in spreading cell death (Figure 2.3.5A).

To test if the cell death inducer can be replaced, several potential inducers were tested in leaves with low *NbRD21* levels. Matching resistant gene (R) and avirulence gene (AVR) couples lead to gene-for-gene interactions, triggering programmed cell death, HR (Gilroy *et al*., 2007). Combinations of *Rx* and *CP*, *Cf4* and *Avr4* as well as *N* and *P50* were used to trigger HR. *TRV::SGT1* plants which cannot develop HR were included in assay to confirm if developed cell death was really HR (Peart *et al*., 2002, Azevedo *et al*., 2006). Although HR develops normally in these plants, none of the HR inducers did promote spreading cell death in *NbRd21* silenced plants (Figure 2.3.5B). Other cell death inducers such as methanol infiltration, mechanical damage, TMV (tobacco mosaic virus) and PVX (Potato virus X) did also not trigger spreading cell death (data not shown).

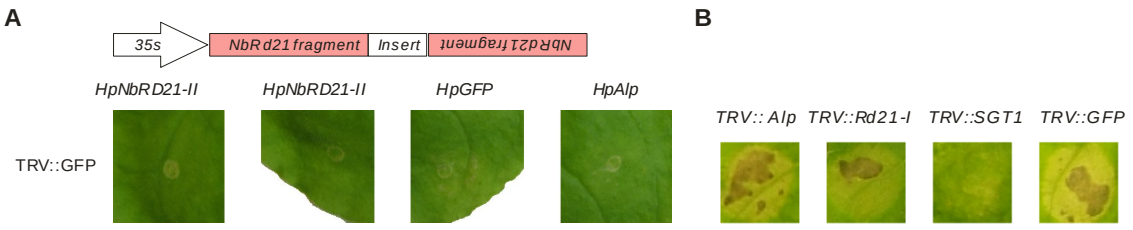

Figure 2.3.5. Uncoupling cell death inducers: TRV-independent transient silencing (even by adding TRV) nor HR inducers do not trigger spreading cell death

(A) Co-infiltration of hairpin silencing constructs with TRV::GFP (full length). Inverted repeat constructs (hp; hairpin), were used as local silencing inducer. Bright field and GFP fluorescence image were taken at 5dpi. **(B)** Infiltration of cell death inducers into systemic leaves of plants infected with TRV constructs. Cell death inducers Rx+CP were infiltrated into systemic leaves of plants. HR insensitive *TRV::SGT1* was used as negative control for confirming the cell death is HR.

2.3.4. Silencing autophagy-related genes pheno-copies *NbRd21* silencing

Liu *et al.* (2005) showed that when autophagy related genes are silenced in *N. benthamiana*, spread of cell death cannot be restricted. This phenotype could be similar to the *TRV::NbRd21* phenotype. Fragments of six autophagy-related genes (*Atg7*, *Atg6*, *Atg3*, *Atg5*, *PI3K* and *Atg8e*) were selected for TRV-based virus-induced gene silencing. *TRV::Atg3* plants showed a retarded growth at 28 dpi and a cell death phenotype at 14 dpi, similar to *TRV:: NbRd21* plants (Figure 2.3.6A). *TRV::Atg6* plants also showed a cell death phenotype, but weaker than *TRV::Atg3* or *TRV::NbRd21* plants (Figure 2.3.6B). *TRV::Atg3* infiltration in mature leaves caused a ring-shaped cell death at 5 dpi, similar to *TRV::NbRd21* (Figure 2.3.6C). Infiltration of *TRV::Atg3* virions to non-inoculated plants initiated cell death (Figure 2.3.6D). Thus, *Atg3* silencing pheno-copies *NbRd21* silencing.

The phenotypic similarities suggested a molecular link between *NbRd21* and autophagy. To investigate that, we monitored *NbRd21* transcript levels and NbRD21 activity in *TRV::Atg3* plants. Transcript levels in systemic leaves of *TRV::Atg3* and *TRV::Atg6* plants were up-regulated when compared to *TRV::GFP* plants (Figure 2.3.6E). Activity-based profiling with DCG-04 on systemic leaves of *TRV::Atg3* and *TRV::Atg6* plants showed a reduced 40 kDa signal of iNbRD21 similar to that of *TRV::NbRd21* plants (Figure 2.3.6F). In contrast, the intensity of the Alp signal is unaltered in *TRV::Atg3*, *TRV::Atg6* and *TRV::NbRd21* plants. This implies that silencing of *Atg3* or *Atg6* leads to a decrease of NbRd21 activity, while the *NbRd21* transcript level is up-regulated, indicating that *Atg3* or *Atg6* silencing hampers NbRD21 function.

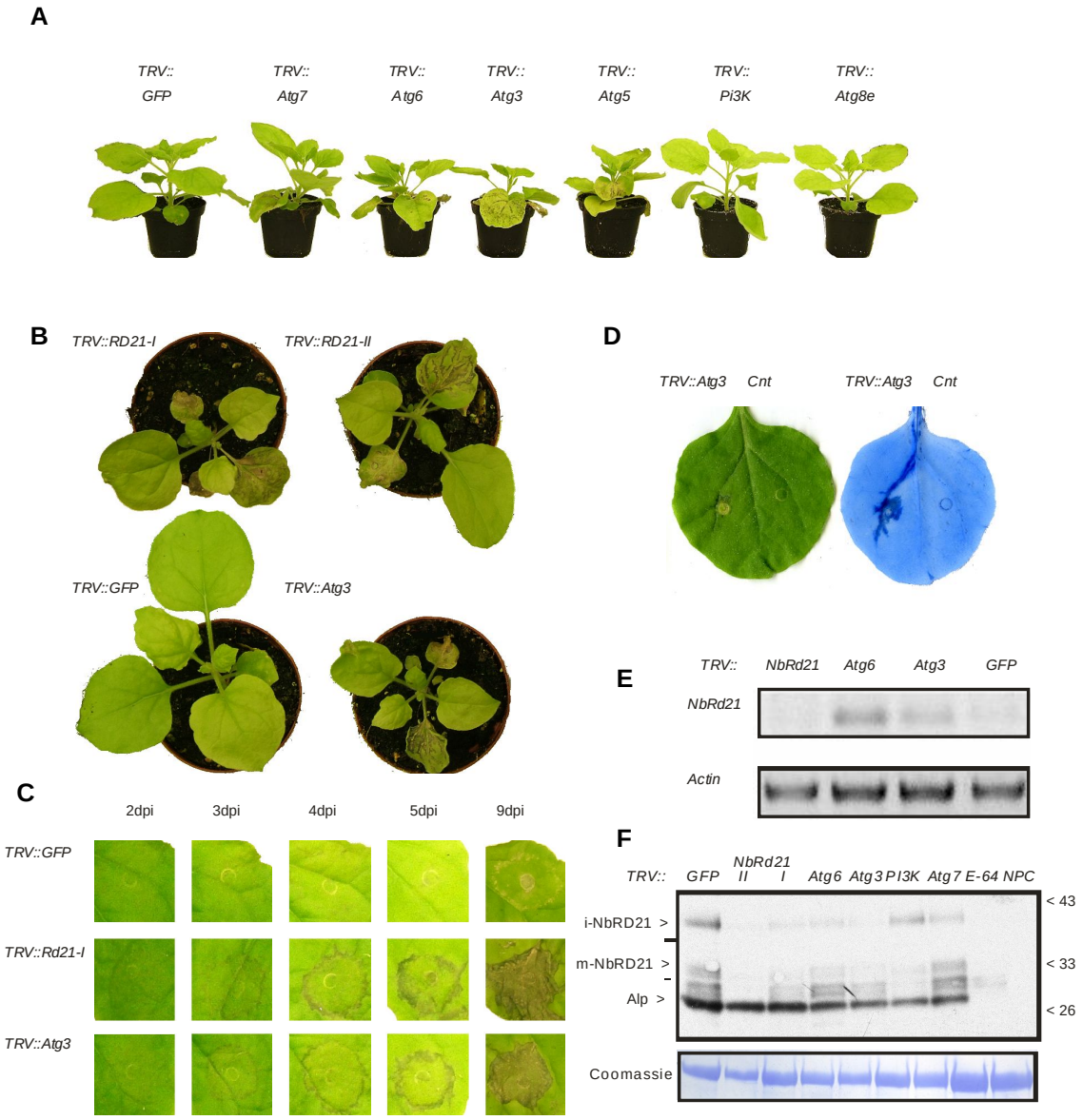

Figure 2.3.7 Analysis of autophagy-related gene silenced plants.

(A) Silencing of some of autophagy-related genes. Fragment of *Atg7*, *Atg6*, *Atg3*, *Atg5*, *PI3K* and *Atg8e* were used for TRV-based silencing constructs. Images were taken at 28dpi. **(B)** Cell death phenotype of *TRV::Atg3* plants compared to *TRV::NbRd21* and *TRV::GFP* plants at 14dpi. **(C)** Infiltration of *TRV::Atg3* into mature leaf. Infiltrated leaves were monitored up to 9dpi. **(D)** *TRV::Atg3* virons inoculated into new leaf (left). Dead cells were stained with Trypan blue at 5 dpi (right).

(E) Transcript analysis of systemic leaves of silenced plants. RNA of *TRV::NbRd21*, *TRV::Atg6*, *TRV::Atg3* and *TRV::GFP* plants were isolated and subjected to semi-quantitative RT-PCR using gene specific primers of *NbRD21* (top) and *actin* (bottom).

(F) DCG-04 protease activity profiles of systemic leaves of silenced plants. Activity-based protein profiling with DCG-04 was performed on systemic leaves, at 28 dpi with various constructs (Top). Corresponding coomassie stained gel is shown as control (Bottom). NP, no probe control; +E-64, addition of excess E-64 to compete DCG-04 labelling. Molecular weight (in kDa) are indicated to the right of the image.

3 Discussion

Here we have shown that Arabidopsis RD21A contributes to resistance to *B. cinerea*. Moreover, it was demonstrated that virus-induced gene silencing of *NbRd21* triggers cell death, probably initiated by Tobacco Rattle Virus. This *TRV::NbRd21*-induced cell death is pheno-copied by silencing autophagy related genes and NbRD21 activity is hampered in *Atg3* and *Atg6* silenced plants. Furthermore, transcript levels of tomato apoplastic-space secreted PLCPs, RCR3 and PIP1, are induced upon BTH treatment and the proteases are under high evolutional selection pressure to diversify.

3.1 Diversifying defence-related PIP1 and RCR3

Although the idea that PLCPs act in biotic stress responses is relatively new (Van der Hoorn and Jones, 2004), transcriptional changes of PLCPs upon abiotic stresses, including drought, cold, ABA, have been reported since decades (Grudkowska and Zagdanska, 2004, Harrak *et al*., 2001, Lohman, *et al*., 1994). Connections of PLCPs to drought stress and senescence have been well described. Good examples are *Sag12* and *AALP* homologues (Lohman, *et al*., 1994, Eason et al., 2005). Both proteases are in vacuole, presumably degrading proteins during senescence. Some PLCPs react to both drought and senescence, but some respond to these conditions independently (Beyene *et al*., 2006).

Our data indicate that PIP1 and RCR3 belong to the class of PR proteins that accumulate during the immune response via SA signalling pathway (Figure 2.2.1). Also during infections with *C. fulvum*, transcript levels of *RCR3* is up-regulated (Kruger *et al*., 2002). Other studies showed that *PIP1* is up-regulated during infection with *Pst* and *P. infestans* (Zhao *et al*., 2003; Tian *et al*., 2007). RCR3 is required for recognition of *C. fulvum* protein Avr2 (Rooney *et al*., 2005). Furthermore, PIP1 is inhibited by cystatin-like Epic2B secreted from *P. infestans* during infection (Tian *et al*., 2007). What is striking was that both BTH induced proteases are inhibited by Avr2 and that both are under diversifying selection (Shabab *et al*., 2008). All variant residues found in PIP1 and RCR3 are at the surface, around the substrate-binding groove, possibly affecting the affinity with inhibitors (Figure2.2.2, Shabab *et al*., 2008). Diversifying selection at the protein-protein interaction surface often occurs in plant-pathogen interactions (Reviewed in Misas-Villamil and Van der Hoorn, 2008). This indicates that BTH-induced proteases are under strong selection pressure caused by pathogen-derived inhibitors. Indeed, a naturally occurring variant amino acid in RCR3 prevents the inhibition by Avr2 (Shabab *et al*., 2008). Taken together these data

demonstrates that biological functions of PLCPs go beyond the degradation of proteins under drought or senescence conditions, as they also seem to act in defence.

3.2 PLCPs in abiotic and biotic stress responses

Previous studies have revealed a number of PLCPs with defence-related roles, including Papain, NbCatB, Mir1 and RD19 (Konno *et al.*, 2004, Gilroy *et al.*, 2007, Pechan *et al.*, 2002, Bernoux *et al.*, 2008). Our data, with increased *Botrytis* susceptibility of Arabidopsis *rd21* mutants, supports us to add RD21A as a new defence-related PLCP (Figure 2.1.2G, 2.1.3F,G). How RD21 is involved in defence to *Botrytis* remains to be determined. One possible interpretation is that RD21 is responsible to restrict cell death. The necrosis induced by *Botrytis* might be restricted in the presence of RD21. However, other necrotrophic pathogens, including *A. brassicicola* and *C. higginsianum*, did not show altered susceptibility on *rd21* mutant plants, suggesting that defence the role of RD21 can be a minor for other necrotrophic pathogens. No changes of transcript levels of *RD21*/*C14* upon BTH treatment were detected (Figure2.2.1, Appendix 1C). This indicates that RD21 transcript accumulation is not mediated via SA signalling pathway. PLCPs, in which involved in defence independent of SA pathway, have already been reported (Zhao *et al.*, 2003). Microarray data indicate that transcript levels of *RD21* do not change by during *Botrytis* infection (Appendix 1C). Here, it is only conclusive that RD21 contribute to defence against *Botrytis* infection, independent from pathogen perception of SA signalling pathway in Arabidopsis.

Other pathogens tested on *rd21* mutants did not exhibit any phenotype. This was unexpected, since the activity of RD21 is induced during infection with avirulent *Pst* and is suppressed during infection with virulent *Pst* of Arabidopsis cell culture. Further studies on potential protease inhibitors of *Pst* revealed a Chagasin-like inhibitor named RIP1 (Kaschani and Van der Hoorn, unpublished). RIP1 inhibits the activity of Arabidopsis RD21 and tomato C14 *in vitro* and is predicted to be secreted by the type II secretion system (Kaschani and Van der Hoorn, unpublished). This suggests that the absence of a phenotype of the *rd21* mutant can be due to the presence of RD21 inhibitors that abolishes RD21 activity in wild-type plants. Yet it is not clear if RIP1 inhibition to RD21 occurs *in vivo* during infection and if the *Pst rip1* knock-out has a reduced bacterial growth on *rd21* mutant plants.

3.3 RD21 redundancy

It has been assumed that other PLCPs may take over the role of RD21,

causing less dramatic phenotypic changes of *rd21* knock-out plants for *Pst* and other pathogens. We first hypothesised that granulin containing PLCPs (RD21B, RD21C and RD21D) may act redundantly to RD21A. This assumption was based on the presence of a granulin domain in RD21B, C and D, a feature that is well conserved across plant species (Schaffer and Fischer, 1990, Linthorst *et al.*, 1993, Tabaeizadeh *et al.*, 1995, Drake *et al.*, 1996, Yamada *et al.*, 2001, Avrova *et al.*, 1999, Chen *et al.*, 2006, Kikuchi *et al.*, 2008). The importance of granulin peptides has been well demonstrated in animal research (Cadieux *et al*, 2005, Cruts *et al.*, 2006). Granulins act as growth hormones that contribute to wound induced defence response (Bateman and Bennett, 1998). We were unsuccessful at obtaining the *rd21C* mutant, though this protease that is rather expressed in roots, making redundancy with RD21 function in leaves less likely.

A second source of redundant proteases that are functionally redundant to RD21 might be the closely related non-granulated versions of RD21A, for example RDL1 (Figure 1.2). Similarly, RDL2 (At3g19400) might act redundant with RD21C (At3g19390), since they are highly homologous and probably evolved from an recent gene duplication. Although many of these proteases were not identified in leaf proteomes of non infected wild-type Arabidopsis leaves (Van der Hoorn *et al.*, 2004), these homologues may require particular stress stimuli to trigger activation.

3.4 RD21 and TRV cause cell death

We demonstrated that virus-induced gene silencing of *NbRd21* leads to retarded growth and cell death, independent from Agrobacterium (Figure2.3.3C, 2.3.4B). However, *NbRd21* silencing alone is not sufficient to trigger cell death. The most likely scenario is that the cell death is triggered by the silencing vector, Tobacco Rattle Virus (TRV). TRV is a well-known plant RNA virus that causes necrosis and wilting of tobacco, causing leaves rattling in the wind, hence the name. The introduction of an extra nucleotide sequence in RNA virus suppresses virulence (Chapman *et al.*, 2008). The same has been observed in case of TRV (Ruiz *et al.*, 1998, Lu *et al.*, 2003). Our data suggest that *NbRd21* silencing enhances TRV symptoms. This necrosis explains also the retardation of plant growth upon *TRV::NbRd21* inoculation.

Cell death caused by TRV and *NbRd21* silencing appeared difficult to uncouple. Although we have detected silencing using *hpNbRd21* constructs, this did not trigger the cell death, even upon additional inoculation with TRV::GFP (Figure 2.3.5A). It has been demonstrated that transient RNAi-based silencing can only silence

locally and transiently, peaking at 6 dpi (Koscianska *et al.*, 2005, Kalantidis *et al.*, 2006). The NbRD21 protein might be too stable to disappear using transient RNAi. This leads to experimental difficulties to synchronise effective silencing and high production of TRV at the same time.

Himber *et al.* (2004) found that silencing is stronger at the border of the silenced region; the formation of ring shaped cell death can be explained by small RNAs produced in the infiltrated region that can move ten cells, causing a ring of silencing around the infiltrated area. Presumably, cell death might have been initiated by TRV at the border of the infiltrated region, where strong silencing occurs. Moreover, Agrobacterium induces biotic stress that may suppress the cell death (Pruss *et al.*, 2008). This might explain the formation of a cell death ring. Generation of transgenic *hpNbRd21 N. benthamiana* plants is in progress and may help to understand the mechanism of how cell death occurs upon *NbRd21* silencing.

3.5 What is the biochemical function of RD21?

So far, many biochemical characteristics of RD21A have been reported. For example, activity of RD21 is enhanced by adding of SDS (Yamada *et al.*, 2001, Halls *et al.*, 2006). However, what the exact biochemical function of RD21 is remains an open question. We recently found that RD21A can also ligate peptides; in cellular extracts, RD21 accepts peptides as donor molecules and ligates them, probably through a thioester intermediate, to unmodified N termini of acceptor proteins, for example oxygen-evolving complex of photosystem II, PsbP (Wang *et al.*, 2008). This occurs in extract at neutral to basic pH. It is yet unknown if this also occurs *in vivo*, since RD21A presumably resides in acidic compartments. The newly identified function of RD21A as a potential peptide ligase may helps us to find its client proteins and unravel the biological role of RD21.

Localization study of RD21A had lead to contrasting data. In case of Arabidopsis, RD21 is transported directly from the ER bodies into the vacuole (Hayashi *et al.*, 2001). Tomato C14, one the other hand, localised in nuclei, chloroplasts and the cytoplasm (Tabaeizadeh *et al.*, 1995). Biochemical assays revealed that both iRD21 and mRD21 are equally active and acidic pH is required for the granulin domain release (Hayashi *et al.*, 2001, Van der Hoorn, *et al.*, 2004). This may suggest that RD21 may act differently in the cells.

There is one report indicating a potential interacting RD21A partners. RD21 from cauliflower caused cleavage of the proform AALP, leading to AALP activation (Halls *et al.*, 2005). This suggests that RD21 might post-transcriptionally regulate

AALP. However, we found that when activity-based profiling was applied to *rd21A* knock-out lines or *NbRd21* silenced plants, active AALP or Alp was detected to the same level as in control plants, indicating that AALP processing can occur without RD21 or NbRD21 (Figure 2.1.1, 2.3.1B). Possibly AALP activation by RD21 activation occurs only *in vitro*. RD21 may also act redundantly with other PLCPs or the activation is specific for cauliflower.

PDI5 is a protein disulfide isomerase which can oxidize, reduce and isomerise disulfide bonds, modulate redox responses and chaperone proteins (Ondzighi *et al*., 2008). PDI5 is expressed in endothelial cells (seed coat layer) about to undergo PCD in developing seeds and its mutation results in fewer non viable seeds in Arabidopsis (Ondzighi *et al*., 2008). A cytological study demonstrated that PDI5 follows the trafficking of RD21 from the ER to the vacuole and PDI5 inhibits RD21 *in vitro*, implying that RD21 contributes to PCD (Ondzighi *et al*., 2008). However, *rd21* mutants did not show retarded seeds development and also the inhibition occurs *in vivo* remains to be answered.

Other potential RD21-regulating proteins are kunitz-type inhibitors and cystatins (Halls *et al*., 2006, Martinez *et al*., 2005). Sequence analysis shows kunitz-type inhibitors and all the cystatins carries signal peptides, except cystain1. Interestingly, drought stress and leaf senescence causes the accumulation of kunitz-type inhibitors in the cells and specific transcript down-regulation of Cystatin-1 (Halls *et al*., 2006, Zimmermann *et al*., 2004). Kunitz-type inhibitors inhibit RD21 activity *in vitro* under acidic conditions and localises in the vacuole where AALP and RD21 accumulate (Halls *et al*., 2006). There are seven cystatins found in Arabidopsis (Martinez *et al*., 2005) and some are already described with their biological functions (Beatrice *et al*., 2003). Similarly, cystain-5 and cystatin-6 inhibitions and selective cystain-1 inhibition to RD21A has been revealed using DCG-04 (Both and Van der Hoorn, unpublished data). Previously a soybean cystatin has been implicated in PCD regulation (Solomon, *et al*., 1999). Therefore, it is well possible that these inhibitors post-translationally regulate the activity of RD21.

3.6 Autophagy and RD21

Autophagy is a dynamic process that involves many proteins with diverse and unique functions (Bassham, 2007, Table 1.1). Of the seven autophagy-related genes silenced, we observed that phenotypes upon silencing of *ATG3* or *ATG6* (*beclin*) resembles the phenotype of *NbRd21* silencing. ATG3 is an E2-like ligase that can ligate the ubiquitin-like ATG8 protein to phosphatidylethanolamine (Yamada *et al*., 2007).

ATG6/beclin is responsible for activating autophagosome formation together with the kinase complexes (Thompson and Vierstra, 2005). Although disruption of autophagy often results in an accelerated senescence phenotype (Hanaoka *et al*., 2002, Bassham, 2007), abolishment of autophagy function can also cause unlimited PCD (Liu *et al*., 2005). We did not observe an accelerated senescence phenotypes neither upon *ATG3* nor upon *NbRd21* silencing. Comparison of *NbRd21* with *ATG3* and *ATG6* silencing phenotypes suggests that the role of *NbRD21* in autophagy is more related to *ATG3* than to *ATG6*. In fact, unlimited spreading of PCD induced by TMV in *ATG6* silenced *N*-transgenic plants could not be observed in *NbRd21* silenced plants (data not shown, Liu *et al*., 2005). This suggests that NbRD21 function is more related to the ATG8 modification than to autophagosome formation, a possible role for RD21 might be ATG8 processing. For example, ATG4 is a cysteine protease that is required for C-terminal processing of ATG8 before the ATG3-mediated ligation (Ketelaar *et al*., 2004). But yet it is not clear if the ATG8 is cleaved directly by ATG4 or indirectly by another protease activated by ATG4 (Tanida *et al*., 2006). Arabidopsis *atg4* mutants display increased chlorosis, accelerated bolting, enhanced dark-induced senescence of detached leaves and reduced seed yield (Yoshimoto *et al*., 2004). Phenotypes of *ATG4*-silenced *N. benthamiana* has not been reported. However, since ATG4 modification to ATG8 occurs before the ATG3 ligation step, abolishment of ATG4 function may result in the same phenotype as *ATG3* silenced plants. The similar phenotypes upon *ATG3* and *NbRd21* silencing suggest *NbRd21* is maybe responsible for ATG4-like ATG8 modification. This can be tested by ATG4 silencing and investigating ATG8 accumulation in NbRD21 silenced plants. Silencing of *ATG8E* did not exhibit the cell death phenotype (Figure 3.3.7A). This is probably due to the presence of many ATG8 homologues in plants (Bassham *et al*., 2006).

The presence of cysteine protease inhibitors can affect, autophagy *in vivo* has been known for decades (Moriyasu and Ohsumi, 1996). In mammalian studies, adding cysteine protease inhibitor leupeptin to cells causes the accumulation of autolysosomes (Kominami *et al*., 1983). Similarly, plant cells treated with E-64 accumulate particles of cytoplasm in membrane bound structures, presumably representing plant autolysosomes (Moriyasu and Ohsumi, 1996). During the final stage of autophagy, autophagic bodies are degraded in the vacuole and also this process is attenuated by E-64 (Thompson and Vierstra, 2005). However, which inhibited cysteine proteases are responsible for these phenotypes has not been determined. Both *in vitro* and *in vivo* DCG-04 labelling showed that RD21 is one of the most prominent proteases in leaves (Figure2.1.1, Van der Hoorn, *et al*., 2004). This suggests that the disturbance of

autophagy by E-64 treatment can be caused by inhibition of RD21. This is supported by our data showing that *ATG3* and *ATG6* silencing resulted in an up-regulation of *NbRd21* transcripts without an increased NbRD21 activity. One explanation is that the transcript levels of *NbRd21* is increased upon *ATG3* and *ATG6* silencing to compensate for the loss of autophagy, but that RD21 cannot accumulate since the autophagy is disturbed. The exact role of RD21 in autophagy will need to be further investigated.

3.7 Perspectives

The findings presented in this study allowed us to understand the some of functional aspects of PLCPs in general and RD21. Yet there are many open questions left. We found that some of tomato PLCPs are involved in SA signalling pathway, however it is not yet clear which PLCPs respond to what abiotic or biotic stimuli for what biological relevance. As we observed, PLCPs, of which are under strong diversifying selection, seemed to play a role in direct recognition of pathogen derived inhibitors. The potential inhibitors secreted by pathogens and the diversifying PLCPs need to be further investigated.

rd21 mutants are more susceptible for *Botrytis* infection. One can assume that if RD21 is responsible for restricting the necrosis spread, the question would be why not other necrotrophic pathogen tested did not display the susceptible phenotype. RNAi RD21C and other PLCPs knock-out line crossed with *rd21ABD* mutant can be tested, if this was due to the redundancy of RD21.

TRV::NbRd21 silencing resulted cell death, probably caused by TRV. Uncoupling of *NbRd21* silencing from TRV is so far unsuccessful. Generation of transgenic *hpNbRd21 N. benthamiana* plants is in progress. This may help us to identify the actual inducer of cell death and to test if the cell death elicitor is replaceable.

Further investigation of the biochemical characteristics of RD21 is required to understand the function of RD21. Analysis of mutated recombinant RD21 is in progress. To understand the RD21 regulation mechanisms, *in vivo* interaction of RD21 previously described *in vitro* inhibitors are going to be tested.

Atg3 silenced plants pheno-copied *NbRd21* silencing. This speculates that *NbRd21* contributes to autophagy. *Atg4* silenced plants can be generated to test, if NbRD21 is involved in ATG8 modifications. Co-localization experiment of NbRD21 and ATG8 is in progress. E-64 caused auto-lysosome accumulation can be tested in *NbRd21* silenced plants, to investigate how NbRD21 contribute to autophagy.

4. Materials & Methods

4.1. Materials

Chemicals and antibiotics

All chemicals and antibiotics were supplied by Sigma (Deisenhofen, Germany), Roth (Karlsruhe, Germany), Merck (Darmstadt, Germany) and Duchefa (Haarlem, Germany). DCG-04 was provided by Dr. Herman Overkleeft (Leiden University, Netherlands) and Dr. Matt Bogyo (Stanford Medical School, USA) and were synthesized as described previously (Greenbaum *et al.*, 2002).

Enzymes

Restriction enzymes were from Fermentas (St.Leon-Rot, Germany) and New England Biolabs (Frankfurt/Main, Germany). Taq polymerase for standard PCR was either from Promega (Mannheim, Germany) or BioBudget (Krefeld, Germany) and high-fidelity polymerase was from Roche (Karlsruhe, Germany). Reverse-transcriptase was from Invitrogen (Karlsruhe, Germany). Ligases were either from Promega (Mannheim, Germany) or Fermentas (St.Leon-Rot, Germany). DNase and RNase were from Roth (Karlsruhe, Germany).

Vectors

Plasmids *pBlueScriptII KS+* (*pBS*) and *pGEM-T* were supplied by Stratagene (Waldbronn, Germany) and Promega, respectively (Mannheim, Germany). *pTRV1* and *pTRV2* vectors were obtained from Dinesh-Kumar (Liu *et al.*, 2002, Lu *et al.*, 2003). *pFK26 CaMV 35S'* promoter containing vector and binary vector *pTP05* were described previously (Shabab *et al.*, 2008).

Kits and primers

Oligonucleotide primers were synthesized by Invitrogen (Karlsruhe, Germany). HPLC purified primers were generated by Sigma (Deisenhofen, Germany). Oligo(dT) primers were from Invitrogen (Karlsruhe, Germany) or Roche (Karlsruhe, Germany). Kits for isolating DNA or RNA were supplied from Qiagen (Hilden, Germany). Plasmid isolation was carried out using kits of Peqlab (Erlangen, Germany) or Macherey-Nagel (Duren, Germany).

All primers are listed in Table 4.1 at the end of the Material and Methods section.

Pathogens

Pseudomonas syringea pv. *tomato* strain *DC3000* (*Pst*) was obtained from Dr. Silke Robatzek and Dr. Jane Parker at the MPIZ (Cologne, Germany). *Pseudomonas syringea* pv. *tomato DC3000* carrying *AvrRpm1*, *AvrRpt2* or *AvrRps4* were all obtained from Dr. Jane Parker. *Colletotrichum higginsianum* and *Hyaloperonospora parasitica* isolates were maintained by members of the Dr. Richard O'Connell and Dr. Jane Parker groups, respectively. *Botrytis cinerea* and *Alternaria brassicicola* were obtained from Dr. Bart Thomma (Wageningen University, Netherlands).

Bacterial strains

Escherichia coli strain DH10B was used for standard cloning. *Agrobacterium tumefaciens* strain GV3101 was used for Agrobacterium-infiltration and plant transformation.

Plant material

All the *Arabidopsis thaliana* work was carried out using ecotype Columbia (Col-0), unless otherwise stated. All the transgenic T-DNA insertion mutants were provided either by the Salk Institute (http://signal.salk.edu/) or by GABI (http://www.gabi.de/) and obtained through NASC (http://arabidopsis.info/), except SAIL_781H05 (*rd21B)* which was kindly provided by Dr. Czaba Koncz (MPIZ, Cologne, Germany). Genotypes were all confirmed by PCR on genomic DNA using gene specific primers (Table.4.1). RD21C screening was performed as described in Rio *et al*., (2002). Arabidopsis Landsberg cell suspension culture was obtained from Sainsbury lab (John Innes centre, Norwich, UK) and maintained according to the method described by Kaffarnik *et al*. (2009). *N. benthamiana* (310A) and tomato (*Solanum lycopersicum* cv. Money-Maker) used in this work were grown at the MPIZ (Cologne, Germany). Accession numbers for tomato relatives, provided by Dr. Klaus Theres are listed below: LA0927 (*S. cheesmaniae*), LA1407 (*S.cheesmaniae*), LA0442 (*S. pimpinellifolium*); LA1930 (*S. chilense*); LA0716 (*S. pennellii*); LA1777 (*S. habrochates*/*hirsutum*); (*S. peruvianum*); LA1028 (*S. schiewlskii*); LA1322 (*S. parviflorum*); and LA1204 (*S. lycopersicum* var *cerasiforme*).

4.2. Methods

Plant growth conditions

Arabidopsis plants used in this work were either grown in long day (16:8 day/night

regime) or short day condition (12:12 day/night regime). In case of plants subjected to pathogen challenges, a short day (day, 24°C; night, 20°C) growth cabinet was used. Four to five-week old plants were used for experiments, unless otherwise stated.
N. benthamiana and tomato were grown in a climate chamber at a 14-h light regime at 18°C (night) and 22°C (day). Four- to six-week old plants were used for experiments. BTH treatment was done by watering 5-week-old tomato plants with 25 mg/ml BTH (Actigard; Syngenta) or water every second day. Samples were taken at 5 days after starting the BTH treatment, unless otherwise indicated.

Plant transformation

Plants were transformed according to the flower dip method described in Clough and Bent (1998) with minor changes. A week before the transformation the primary bolts of plants were clipped and a day before transformation plants were watered and packed in a plastic bag to create high humidity. 500 ml of overnight grown Agrobacterium culture, supplemented with 30 mg/l of rifampicin and kanamycin, was centrifuged and the bacterial pellet resuspended in medium containing 2.3 g/l MS medium and 5% sucrose at an OD_{600} of 1. After adding 0.03% Silwet L-77, flower buds were soaked into the inoculums for ten seconds and plants were covered with a plastic bag overnight, placed horizontally.

Selection of transformants

Successful transformants were selected on MS media (1.5% agar, 0.05% MES, 1% sucrose and 0.44% MS salt, pH 5.6) supplemented with 100mg/l kanamycin. Seed surface sterilization was performed according to the vapour-phase method that produces chlorine gas by adding hydrochloric acid into commercial bleach in 1:10 dilution (described at http://plantpath.wisc.edu/~afb/vapster.htm). Two to three-week old plants showing kanamycin resistance were transferred to soil and T-DNA presence was confirmed by PCR using insert specific primers (Table. 4.1).

Genomic DNA preparation

Genomic DNA was isolated from plants using method described previously (Thorlby *et al.*, 2004). Leaf materials were ground in 400 µl Edward buffer (200 mM Tris pH 7.5, 250 mM NaCl, 25 mM EDTA, 0.5% SDS). After centrifugation, the supernatant was transferred to a new tube and mixed with an equal volume of isopropanol (normally 300 µl). The DNA pellet was precipitated by five minutes centrifugation and dried after removing the supernatant. DNA was dissolved in 100 µl of H_2O without vortexing.

Crosses

Every flower organs of the acceptor except the carpel was removed from flower buds using fine forceps. Mature flowers of the donor were selected and used to pollinate the acceptor carpel. The pollinated acceptor was wrapped with clean film until the seeds were ready to harvest.

Pathogen assays

***Pseudomonas syringea* pv. *tomato* growth assay**

Pst DC3000 (with and without *Avr* genes) was inoculated by spraying as described previously (Katagiri *et al.* 2002). The optical density of bacteria in the spray inoculums was OD_{600} 0.01 to 0.05. Bacterial counts were performed according to the method described previously (Tornero and Dangl, 2001). Photographs were taken at 4 dpi.

***Botrytis cinerea* and *Alternaria brassicicola* pathogen assays**

Droplet inoculation of spores was performed as described previously (Thomma *et al.*, 1998). 5 µl of spore suspension (10^5 spores/ml) was inoculated on each mature leaves of 4-week old plants. Percentage of fungal infection (fungal out-growth) were scored and photographed at 5dpi.

***Colletotrichum higginsianum* pathogen assay**

A *Colletotrichum higginsianum* spore suspension was diluted to 10^3 spore/ml and 5 µl droplets were inoculated on leaves of 5-week old plants. Percentage of fungal infection (fungal out-growth) were scored at 5 dpi. To perform spray inoculation, the spore suspension was diluted to 10^4 spore/ml and sprayed onto 3-week old plants. Pictures were taken at 7 dpi.

***Hyaloperonospora parasitica* growth assay**

Spray inoculation of *Hyaloperonospora parasitica* was performed according to the method described previously (Parker *at al.*, 1993). The number of spores were counted using haemocytometer and were calculated by the formula: (number of spores x dilution factor)/(counted area x chamber depth).

RNA isolation, cDNA synthesis and analysis and (quantitative) RT-PCR

Total RNA was isolated from tissues frozen in liquid nitrogen using the RNeasy Plant mini kit (QIAGEN) according to the manufacturer's guidelines. DNase treatment was done before the RNA concentration was measured. cDNA was synthesised using

Superscript II reverse transcriptase and Oligo dT primers. Gene-specific primers are summarized in Table 4.1. Variant nucleotide analysis was performed as described in Shabab *et al*. (2008). Structural models of PIP1 and RCR3 were created as described previously (Shabab *et al*., 2008).

For real-time RT-PCR, gene-specific primers were designed using Pearl Primer software (Table 4.1) (Marshall, 2004). Reaction mixtures for SYBR green (Roche) real-time RT-PCR were made as described previously (Karsai *et al*., 2002). DNA synthesis was recorded with the IQ5 Multicolour Real Time PCR detection system (BioRad). Threshold cycles were recorded in triplicate over five independent biological samples, corrected for the Ct of ubiquitin (Rotenberg *et al*., 2006) and subjected to statistical analysis following the guidelines of the manufacturer (BioRad).

Cloning for VIGS

Arabidopsis RD21A granulin domain amino acid sequence was used for tBLASTn search of the TIGR *N. benthamiana* cDNA database (http://plantta.jcvi.org/) to find two *RD21A*-like granulin containing genes in *N. benthamiana*: *TC7740* (*NbRd21-I*) and *EST748747* (*NbRd21-II*). *NbAlp* (*TC7311*) was found by the same procedure using Arabidopsis AALP protein sequence as template. Several 300 bp regions were selected from the cDNA templates and primers were designed carrying restriction sites *BamHI* (5' end) and *EcoRI* (3' end) (Table 4.1). *N. benthamiana* leaf cDNA was used to amplify the fragments. Cloning vector *pBlueScript II KS+* (*pBS-II*) was digested with restriction enzymes *EcoRI* and *BamHI* and treated with alkaline phosphatase. PCR products were digested and ligated into *pBS-II* and the plasmids were transformed into *E. coli*. Successful clones, validated by nucleotide sequencing, were digested using the same restriction enzymes for shuttling into the *pTRV2* binary vector (Liu *et al*. 2002). Inserts in the *pTRV2* plasmid were confirmed by PCR using vector specific primers.

Fragments of autophagy-related genes were cloned into *pTRV2* through the procedure as described above. The template selection was carried out using Arabidopsis cDNA sequences of *ATG7* (AT5G45900), *ATG6* (AT3G51840), *ATG3* (AT5G61500), *ATG5* (AT5G17290) and *ATG8E* (At2g45170) to find *N. benthamiana* cDNA sequences of AY701319, AY701316, AY701318, EB440576 (*N. tabacum*) and EH369475, respectively. *NcoI-BamHI* restriction sites were used to clone all the fragments into the *pTS49* cloning vector (*pBluescriptII* containing *HindIII*::35S::*NcoI-SalI-BamHI-XhoI* between *HindIII-XhoI* sites). Primer sequences are listed in Table 4.1). All the fragments were shuttled into *pTRV2* using *EcoRI-BamHI* sites.

***Agrobacterium* infiltration of virus-induced gene silencing construct**

pTRV2 plasmids were transformed into *Agrobacterium tumefaciens* strain GV3101. Infiltration of *Agrobacterium* was performed as described previously (Shabab *et al.*, 2008). Overnight grown *Agrobacterium* cultures carrying *pTRV1* or *pTRV2* were centrifuged and bacteria were resuspended in infiltration buffer (10 mM MES pH 5, 10 mM $MgCl_2$, 1 mM acetosyringone). Cultures were incubated for two to four hours at room temperature. OD_{600} was adjusted to 2 and *pTRV2*-containing cultures were mixed with *pTRV1*-containing cultures. Cultures were infiltrated into two leaves of 4-week old young *N. benthamiana* plants. Inoculated plants were used at three to six weeks after infiltration. *TRV::GFP* (provided by M. Joosten) was used as negative control and by the bleaching phenotype of *TRV::PDS* (provided by M. Joosten) was used as a positive control for silencing.

Co-infiltration of GFP and TRV vectors

For making binary *35S::GFP* constructs, template GFP was obtained from the Panstruga group (MPIZ, Germany). The GFP-encoding fragment was cloned into *pFK26* using primers, GFP-F and GFP-R (See Table 4.1 for sequences), using *XhoI-PstI* restriction sites and shuttled into binary vector *pTP5* using *HindIII-EcoRI* sites (Shabab *et al.*, 2008). After transformation of *Agrobacterium*, cultures were prepared as described above and mixed with cultures carrying *pTRV1* and *pTRV2* in a 1:1 ratio. Images were generated using the fluorescence microscope.

Trypan blue staining

Trypan blue staining was performed as described previously (Parker *et al.*, 1993). Whole *N. benthamiana* leaves were boiled in Trypan blue solution (30 ml lactophenol, 10 mg trypan blue, 30 ml ethanol), destained with chloral hydarate solution (2.5 g/ml chloral hydrate in H_2O) for more than two days and photographed.

Generation of "hairpin" constructs

The same regions of nucleotide sequence as the *pTRV2* constructs were chosen to construct *hairpin* (*hp*)*NbRD21-I*, *hpNbRD21-II*, *hpNbAlp* and *hpNbCatB*. All the primers used in this work are listed in Table 4.1. A PCR fragment, containing *BamHI* site at 3' and *XhoI* site at 5' ends, of Arabidopsis *A5tg15070* (part of first intron) was cloned into a *pGEM-T* vector to construct *pFK29*. To clone sense-fragment, PCR fragments of each gene were cloned into *pFK26* using *NcoI-BamHI*, resulting in *pTSX1*. In case of antisense construct, *PstI::XhoI-XbaI* sites were introduced by PCR and PCR

products were cloned into *pFK29* using *PstI-XbaI* to make *pTSX2*. Donor vector *pTSX2* was then digested with *BamHI* and *PstI* and combined with acceptor vector *pTSX1* to form *pTShp.* The insert of *pTShp* was shuttled into binary vector *pTP5*. Infiltration was performed as described previously (Shabab *et al.*, 2008).

Infiltration of virons

Leaf disks (1 cm^2) of *pTRV* inoculated plants (4 weeks after infiltration) were ground in 2 ml H_2O and centrifuged at 5000 rpm. 1 ml of supernatant was infiltrated into leaves of 6-week old fresh *N. benthamiana* plants. Pictures were taken at 5 dpi and leaves were stained with Trypan blue as described above.

Western blot and Activity-based protein profiling

Activity-based protein profiling was performed as described previously with minor changes (Van der Hoorn *et al.,* 2004). Protein extraction was performed in H_2O containing 10 µM DTT and the extract was centrifuged. 450 µl of supernatant was mixed with 50 µl 10x buffer (250 mM NaAc (pH 6), 10 µM DTT or 100 mM fresh L-cysteine) and 1 µl of DCG-04 (1 mg/ml in DMSO). For the negative control, 3 µl of 1 mM E-64 was added for compete DCG-04 labelling. After four to five hours incubation, 1 ml cold acetone was added, vortexed and centrifuged. Supernatant was then discarded and pellet was washed with 500 µl 70% cold acetone. Pellets were dried at room temperature and resuspended in 50 µl SDS loading buffer. Samples were loaded onto polyacrylamide gel (either 12 or 15%) and proteins were transferred to PVDF membranes. For detecting biotinylated proteins the membrane was incubated with Ultrasensitive streptavidin-HRP (Sigma, dilution of 1:3000) and signals were detected using SuperSignal Femto/Pico substrate (Thermo Fisher Scientific, Bonn, Germany) on X-ray films (Kodak, Germany).

Table 4.1 Primers

Name	Primer sequence (5'-3')	Description
GABI_401H08f	AGACCTCCGTTACAACCTTCG	Screening GABI_401H08
GABI_401H08r	CTCCTACGACGAGAAACATGG	
GABI_792G08f	CTGAAGAAGAAATGGGGTTCC	Screening GABI_792G08
GABI_792G08r	CAACAACATCAGCTTACAACAAAAC	
SAIL_781H05-f	AATCTACGAAGCGTGGATGG	Screening SAIL_781H05
SAIL_781H05-r	CAGGATTTGAGGGATTTTTCC	
SALK_1384831f	CAATGCTGGCTGTAATGGTG	Screening SALK_1384831
SALK_1384831r	CAGCATTTCCATGAGAAGCA	
RD21C1f	GTTAGCGTCGTCAAGAAACTACTCTG	Screening D21C1
RD21C1r	GACGAGGAAAGTAGTAATACCGAGAG	
SALK_10938f	GATCCCATGGCTCTTTCTTCACCTTCAAGAATCC	Screening SALK_10938
SALK_10938r	GATCCTGCAGTCACTTAGTTTTGGTGGGGAAAGAAGCC	
SALK_124030f	GATCCCATGGCTTTAAAACATATGCAAATCTTTCTC	Screening SALK_124030
SALK_124030r	GATCCTGCAGTCATATAGTTGGGTAAGATGCTTTCATGG	
SALK_31088f	GATCCCATGGATCGTCTTAAACTTTATTTCTCCG	Screening SALK_31088
SALK_31088r	GATCCTGCAGTTAATGGGCGGTGGTTGAGACGGTGGC	
SALK_75550f	GATCCCATGGCTGCGAAAACAATCCTATCATCAG	Screening SALK_75550
SALK_75550r	GATCCTGCAGTCAAGCCACAACGGGGTATGATGC	
SALK_084789f	GAAGCCTCAATAGCCACACTG	Screening SALK_084789
SALK_084789r	TATGGCTTTTTCTGCACCATC	
SALK_088620f	ATAGGGTTGTCTGCCCAGTTC	Screening SALK_088620
SALK_088620r	TAGAACATGACGGGACTGTCC	
SALK_019630f	TTGTGTGTGTGTTGACTGC	Screening SALK_019630
SALK_019630r	AAAACTTACATCACCCCAGCC	
SALK_089030f	CGTTGGTCACACATAGTGCAG	Screening SALK_089030
SALK_089030r	GACAATACTGGTTGCTCGCAC	
SALK_110946f	ACCAAAACCGCAAAGTAATCC	Screening SALK_110946
SALK_110946r	TCTAAGACATATGAAGGGGAAATG	
SALK_063455f	AACGGTAAAAGCAACCTCGAC	Screening SALK_063455
SALK_063455r	TGCCACCGTGAGTTTATTATC	
SALK_151526f	AACCAGAAGATCATCTGAAGTGG	Screening SALK_151526
SALK_151526r	ATCACTGTCCGACAGGTTCTG	
LBa1	TGGTTCACGTAGTGGGCCATCG	T-DNA confirmation primer
LBb1	GCGTGGACCGCTTGCTGCAACT	
r112-promf	GGAGAGGACCATTTGGAGAGGACACGT	35's specific primer
r113-termr	GATTAGCATGTCACTATGTGTGCATCC	

Name	Primer sequence (5'-3')	Description
r114-binf	TAGGTTTACCCGCCAATATATCCTGTC	pTP05 specific primer
r115-binr	TTCTGTCAGTTCCAAACGTAAAACGGC	
r016-TC1850f1	GATCGGATCCGTTACTGAAAAATGGGAAGCACAC	TRV::NbRd21-Iα cloning
r017-TC1850r1	GATCGAATTCCCAACCAAATGATCTGAGTTTGAC	
r018-TC1850f2	GATCGGATCCTCTGAACAAGTTTGCTGATATGAG	TRV::NbRd21-Iβ cloning
r019-TC1850r2	GATCGAATTCGTCCACCATCACAGCCAGTATTG	
r020-TC1850f3	GATCGGATCCCCCTGCTTTTGAGTGGGTGATG	TRV::NbRd21-Iγ cloning
r021-TC1850r3	GATCGAATTCTAGTACTGCATGGGATAAGTC	
r028-EST747f7	GATCGGATCCACCCCCTCCACCACCTTCTCCG	TRV::NbRd21-II cloning
r029-EST747r7	GATCGAATTCCTGGCTCTTTAGTGCTTGTACTCC	
r030-EST747f8	GATCGGATCCGGTGGACGAAACTCTGAAATGG	NbRd21-II RT-PCR
r031-EST747r8	GATCGAATTCTTTATTCAAGAATGTACACAGCG	
r032-TC9934f9	GATCGGATCCGGCCGGATGGAAAGCTGCACTG	TRV::CatB cloning
r033-TC9934r9	GATCGAATTCTTGCTGACAGAGAGATATTCAAGCC	
r034-TC9934f10	GATCGGATCCCCGATCCACACAGTATCATGAC	CatB RT-PCR
r035-TC9934r10	GATCGAATTCGGCTGAAGGCAATCCTGCAACCAC	
r036-TC7311f11	GATCGGATCCGAGGTACGAGACAGTTGAGGAG	TRV::Alp cloning
r037-TC7311r11	GATCGAATTCCCAGCAAGATCCGCACTTGCCCTGG	
r038-TC7311f12	GATCGGATCCCATATCCATACACCGGCAAGAATGGC	NbAlp RT-PCR
r039-TC7311r12	GATCGAATTCCCCAATCTGCTCCCCATGAATTCTTC	
r040-pTRV2f	GTTACTCAAGGAAGCACGATGAGC	TRV specific primer
r041-pTRV2r	GTCGAGAATGTCAATCTCGTAGG	
NB03-ATG7F2	GATCCCATGGACATTGCCTTCGCTGAATCT	TRV::ATG7 cloning
NB04-ATG7R2	GATCGAATTCATGTCCAGGCATCGGAATAG	
NB05-ATG6L1	GATCCCATGGCAGTTTGGGAAGGCTATGGA	TRV::ATG6 cloning
NB06-ATG6R1	GATCGAATTCTCCCTGTTAACATCTTCAACCTC	
NB07-ATG6L2	GATCCCATGGCATCAGGAAGAGAGAGATGCAA	TRV::ATG6 cloning
NB08-ATG6R2	GATCGAATTCGAAACTTTGGCCGGAAATG	
NB09-ATG3L1	GATCCCATGGAAGGCGTTCTCAGCATCAAT	TRV::ATG3 cloning
NB10-ATG3R1	GATCGAATTCGCAAGTTGTCATCCTCGTCA	
NB23-ATG5L2	GATCCCATGGCTCCCCCTGCTCTGATTTTA	TRV::ATG5 cloning
NB24-ATG5R2	GATCGAATTCACTTTGCACTATCTTCGCCTTC	
NB25-ATG8EL	GATCCCATGGGCTGCTCGGATTAGGGAAA	TRV::ATG8e cloning
NB26-ATG8ER	GATCGAATTCCCCGAATGTGTTTTCTCCAC	
r152-ubif	CGTGAAAACCCTAACGGGGAAGACG	Ubiquitin RT-PCR
r153-ubir	ATCGCCTCCAGCCTTGTTGTAAACG	
r154-actf	ATGAAGCTCAATCCAAGAGGGGTATC	NbActin RT-PCR
r155-actr	CTCCTGCTCATAGTCAAGAGCCAC	

Name	Primer sequence (5'-3')	Description
r157-TRVCPf	ATGGGAGATATGTACGATGAATC	TRV specific primers
r158-TRVCPr	TTCAACTCCATGTTCTCTAACGAAG	
r159-NbBeclinf	ATGACGAAAAATAGCAGCAGTAGTAC	TRV::ATG6 RT-PCR
r160-NbBeclinr	ACAGTGATGGTGGAGTGAAACCCAG	
r161-NbAtg3f	GAAGAGGAGGACATACCTGACATGGGAG	TRV::ATG3 RT-PCR
r162-NbAtg3r	CTACCAAGGATCAAAGTCCATGGTG	
r163-NbAtg7f	TCCCTGCTTTGGTGCTTGATCCTCG	TRV::ATG7 RT-PCR
r164-NbAtg7r	AAGGCTGATGCACCTCGAAACCTTC	
GFP-F	ATGCTCGAGGTGAGCAAGGGCGAGGAGC	GFP cloning
GFP-R	ATGGGTACCCTGCAGGGATCCTTACTTGTACAGCTCGTCC	
T1S1-18x1	GATCCCATGGTCTGAACAAGTTTGCTGATATGAG	hpNbRD21-II pTSX1 cloning
T1S2-19x1	GATCGGATCCGTCCACCATCACAGCCAGTATTG	
T1S3-18x2	GATCCTCGAGCTGCAGTCTGAACAAGTTTGCTGATATGAG	hpNbRD21-II pTSX2 cloning
T1S4-19x2	GATCTCTAGAGTCCACCATCACAGCCAGTATTG	
T1S5-20x1	GATCCCATGGCCCTGCTTTTGAGTGGGTGATG	hpNbRD21-II pTSX1 cloning
T1S6-21x1	GATCGGATCCTAGTACTGCATGGGATAAGTC	
T1S7-20x2	GATCCTCGAGCTGCAGCCCTGCTTTTGAGTGGGTGATG	hpNbRD21-II pTSX2 cloning
T1S8-21x2	GATCTCTAGATAGTACTGCATGGGATAAGTC	
T2S1-28x1	GATCCCATGGACCCCCTCCACCACCTTCTCCG	hpNbRD21-II pTSX1 cloning
T2S2-29x1	GATCGGATCCTAACTTGTATTTGGCTATTCTTC	
T2S3-28x2	GATCCTCGAGCTGCAGACCCCCTCCACCACCTTCTCCG	hpNbRD21-II pTSX2 cloning
T2S4-29x2	GATCTCTAGATAACTTGTATTTGGCTATTCTTC	
T2S5-32x1	GATCCCATGGGGCCGGATGGAAAGCTGCACTG	hpNbCatB pTSX1 cloning
T2S6-33x1	GATCGGATCCTTGCTGACAGAGAGATATTCAAGCC	
T2S7-32x2	GATCCTCGAGCTGCAGGGCCGGATGGAAAGCTGCACTG	hpNbCatB pTSX2 cloning
T2S8-33x2	GATCTCTAGATTGCTGACAGAGAGATATTCAAGCC	
T3S1-36x1	GATCCCATGGGAGGTACGAGACAGTTGAGGAG	hpNbAlp pTSX1 cloning
T3S2-37x1	GATCGGATCCCCAGCAAGATCCGCACTTGCCCTGG	
T3S3-36x2	GATCCTCGAGCTGCAGGAGGTACGAGACAGTTGAGGAG	hpNbAlp pTSX2 cloning
T3S4-37x2	GATCTCTAGACCAGCAAGATCCGCACTTGCCCTGG	
r110f	ATGGCCTCGAGCAGCTCAACTCTCACCATATCC	C14 start, RT-PCR
r057r	AGCTGGATCCTCAAGAACTGCTCTTCTTTCCTCC	C14 stop, RT-PCR
r142f	CTTGGGAACGAAGAGTTCCGGTGACCGG	C14 sequencing
r143f	AAGCTGGTGGCAGAGACTTCCAGCACTAC	
r070f	AGCTCCATGGCTTCCAATTTTTTCCTCAAG	PIP1 start, RT-PCR
r071r	CCCCGGATCCTCAAGCAGTAGGGAACGACGCAACC	PIP1 stop, RT-PCR
r144f	TCATTTATGGGGCTCGACACTTCATTAC	PIP1 sequencing
r072f	AGCTCCATGGCTATGAAAGTTGATTTGATG	RCR3 start

Name	Primer sequence (5'-3')	Description
r073r	AGCTCTCGAGCTATGCTATGTTTGGATAAGAAGAC	RCR3 stop
r145f	ACTGGATTAAACATACCTAATTCATATC	RCR3 sequencing
r184f	TGAAGACATTAAATGCAAGCTTCTTACAACAATATTC	RCR3 RT-PCR
r187r	AAGTTCCTCCCGCGTAAAACTGTAAATCTTGGCTAGC	
r098f	ATGGCCTCGAGCTCGCTCGTATTGATTCTCGTCG	CYP3 start, RT-PCR
f345r	AAACTGCAGTTAGGCAACGATTGGGTAGGATGC	CYP3 stop, RT-PCR
r146f	GGTATCAATGAGTTTACCGACCTAAC	CYP3 sequencing
r064f	AGCTCTCGAGATGTCACGCTCCTCAGTCCTATTGG	ALP start, RT-PCR
r095r	AGCTCTGCAGTCAGGCAACGACAGGGTAGGATGCACAAG	ALP stop, RT-PCR
r147f	GGGATGAGTTCCGTCGAGTGAAGTTGC	ALP sequencing
r066f	AGCTCCATGGAGCACATAGCCACTTTTTTGC	CatB1 start, RT-PCR
r067r	CCCCTGCAGTTAGTGTTTAGTTGAAGAATTAGC	CatB1 stop, RT-PCR
r148f	GCGCCTTCTTGGAGTTAAGCCCACAAG	CatB1 sequencing
r068f	AGCTCCATGGCCTTGACTTTGAAGTC	CatB2 start, RT-PCR
r069r	AGCTGGATCCCTACATTGAGGCATCAAGGACAGC	CatB2 stop, RT-PCR
r150f	AAGCGCCTTCTTGGAGTTAAGCCTGCA	CatB3 sequencing
r154f	ATGAAGCTCAATCCAAGAGGGGTATC	actin RT-PCR
r155r	CTCCTGCTCATAGTCAAGAGCCAC	
r188f	ATAGACGATACTTTAATAAGGACGTTCTCC	PR1 RT-PCR
r189r	TTGTTACTCACTTGTCTCATGGTATTAGCC	
r194f	CAAAACATAAACTGGGATTTAAGAACTGC	PR4 RT-PCR
r195r	TTTATTATAGTAATGATGATATATGACAC	
RT19f	AATATGCTGATCTGACCACTG	PIP1 real time PCR
RT18r	CCAACAACATCCACATACAC	
RT20f	TACAAGCCGTAACTAAACAG	RCR3 real time PCR
RT21r	TCATATACCCATTCTCACCC	
RT01f	CTCATCTTCTCCACCTTATCC	C14 real time PCR
RT02r	GTTCTGTTCGTCTATGTATCTC	
RT24f	AAGGACTATCATACAAACTCGG	CYP3 real time PCR
RT25r	GGCTAACAATACCATCTTTCC	
RT05f	GTGTCAATAAGTTTACCGACC	ALP real time PCR
RT06r	CAATACCAGTTTCCCTCCAG	
RT11f	TTTCGCTCACTACAAGTCTG	CatB1 real time PCR
RT12r	ACTCGTTTGTTCCTCTTCTG	
RT15f	TTCCTGTTCTAACTCATCCA	CatB2 real time PCR
RT16r	GGATACAGAAACGATCAGAC	
Ubi3f	GCCGACTACAACATCCAGAAGG	ubiquitin real time PCR
Ubi3r	TGCAACACAGCGAGCTTAACC	

Appendix 1. Microarray anaysis of 31 PLCPs and autophagy-related genes in Arabidopsis.

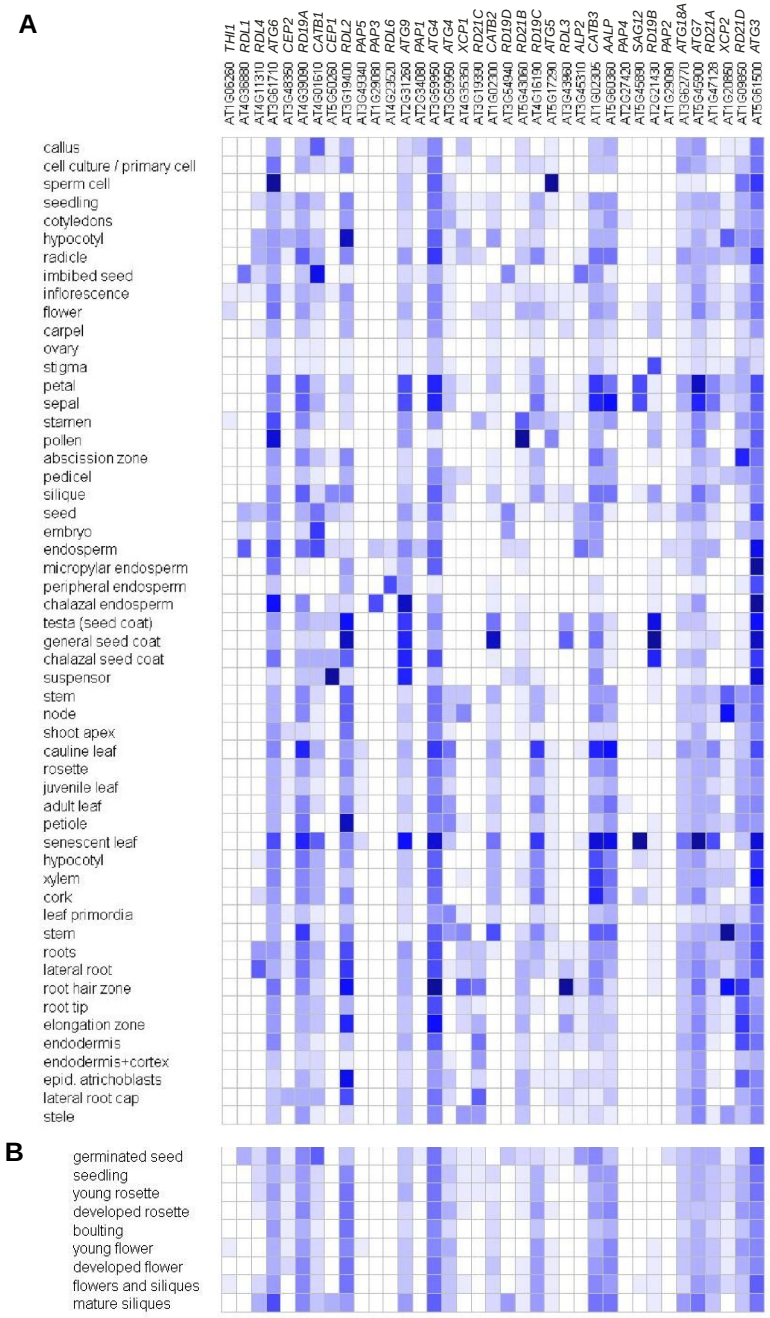

The cluster analysis of microarray data generated at Geneinvestigator (Zimmermann *et al*., 2004). Each column represents a gene. **(A)** each line represents complied microarray experiments demonstrating the expression of the gene in different organ of Arabidopsis. **(B)** each line represents complied microarray experiments showing the expression of the gene in developmental stages. Blue indicates the gene is up-regulated.

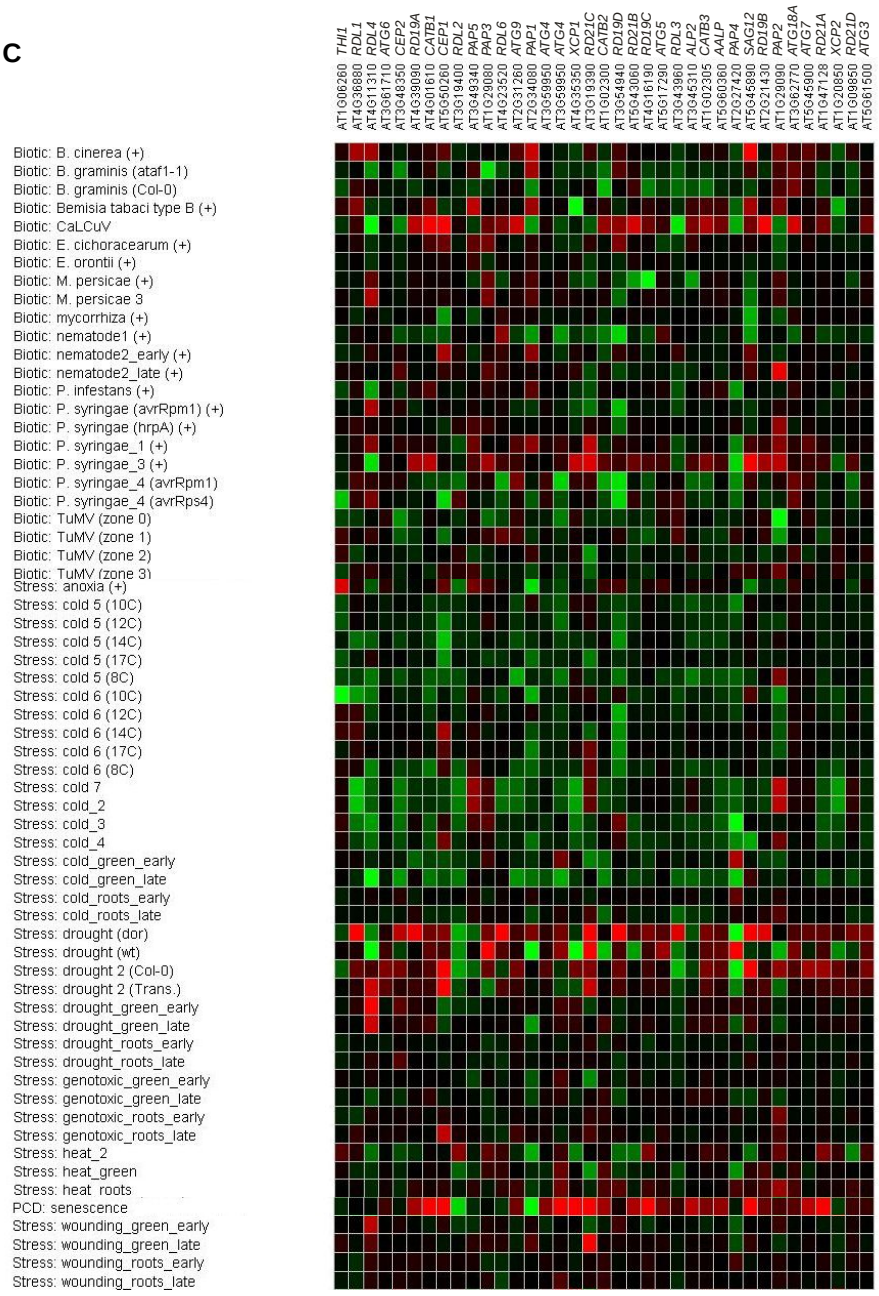

(C) The cluster analysis of microarray data generated at Geneinvestigator (Zimmermann *et al*., 2004). Each column represents a gene. Each line represents complied microarray experiments in which the expression pattern after given treatment is described left side. Green colour indicates that the gene is down-regulated and red indicates the gene is up-regulated.

C

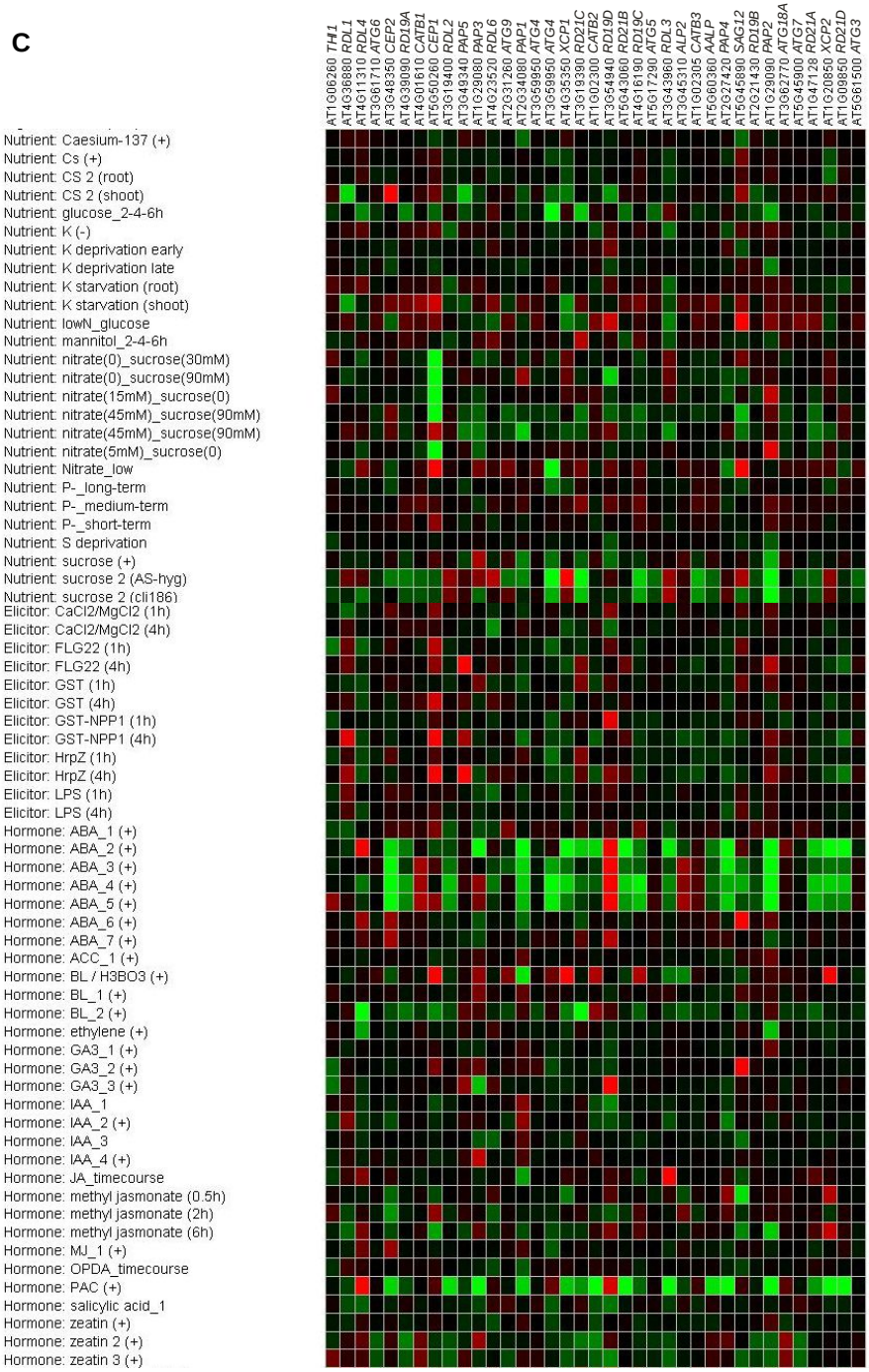
AT1G06260 THI1
AT4G36880 RDL1
AT4G11310 RDL4
AT3G61710 ATG6
AT3G48350 CEP2
AT4G39090 RD19A
AT4G01610 CATB1
AT5G50260 CEP1
AT3G19400 RDL2
AT3G49340 PAP5
AT1G29080 PAP3
AT4G23520 RDL6
AT2G31260 ATG9
AT2G34080 PAP1
AT3G59950 ATG4
AT3G59950 ATG4
AT4G35350 XCP1
AT3G19390 RD21C
AT1G02300 CATB2
AT3G54940 RD19D
AT5G43060 RD21B
AT4G16190 RD19C
AT5G17290 ATG5
AT3G43960 RDL3
AT3G45310 ALP2
AT1G02305 CATB3
AT5G60360 AALP
AT2G27420 PAP4
AT5G45890 SAG12
AT2G21430 RD19B
AT1G29090 PAP2
AT3G62770 ATG18A
AT5G45900 ATG7
AT1G47128 RD21A
AT1G20850 XCP2
AT1G09850 RD21D
AT5G61500 ATG3
Nutrient: Caesium-137 (+)
Nutrient: Cs (+)
Nutrient: CS 2 (root)
Nutrient: CS 2 (shoot)
Nutrient: glucose_2-4-6h
Nutrient: K (-)
Nutrient: K deprivation early
Nutrient: K deprivation late
Nutrient: K starvation (root)
Nutrient: K starvation (shoot)
Nutrient: lowN_glucose
Nutrient: mannitol_2-4-6h
Nutrient: nitrate(0)_sucrose(30mM)
Nutrient: nitrate(0)_sucrose(90mM)
Nutrient: nitrate(15mM)_sucrose(0)
Nutrient: nitrate(45mM)_sucrose(90mM)
Nutrient: nitrate(45mM)_sucrose(90mM)
Nutrient: nitrate(5mM)_sucrose(0)
Nutrient: Nitrate_low
Nutrient: P-_long-term
Nutrient: P-_medium-term
Nutrient: P-_short-term
Nutrient: S deprivation
Nutrient: sucrose (+)
Nutrient: sucrose 2 (AS-hyg)
Nutrient: sucrose 2 (cli186)
Elicitor: CaCl2/MgCl2 (1h)
Elicitor: CaCl2/MgCl2 (4h)
Elicitor: FLG22 (1h)
Elicitor: FLG22 (4h)
Elicitor: GST (1h)
Elicitor: GST (4h)
Elicitor: GST-NPP1 (1h)
Elicitor: GST-NPP1 (4h)
Elicitor: HrpZ (1h)
Elicitor: HrpZ (4h)
Elicitor: LPS (1h)
Elicitor: LPS (4h)
Hormone: ABA_1 (+)
Hormone: ABA_2 (+)
Hormone: ABA_3 (+)
Hormone: ABA_4 (+)
Hormone: ABA_5 (+)
Hormone: ABA_6 (+)
Hormone: ABA_7 (+)
Hormone: ACC_1 (+)
Hormone: BL / H3BO3 (+)
Hormone: BL_1 (+)
Hormone: BL_2 (+)
Hormone: ethylene (+)
Hormone: GA3_1 (+)
Hormone: GA3_2 (+)
Hormone: GA3_3 (+)
Hormone: IAA_1
Hormone: IAA_2 (+)
Hormone: IAA_3
Hormone: IAA_4 (+)
Hormone: JA_timecourse
Hormone: methyl jasmonate (0.5h)
Hormone: methyl jasmonate (2h)
Hormone: methyl jasmonate (6h)
Hormone: MJ_1 (+)
Hormone: OPDA_timecourse
Hormone: PAC (+)
Hormone: salicylic acid_1
Hormone: zeatin (+)
Hormone: zeatin 2 (+)
Hormone: zeatin 3 (+)

C

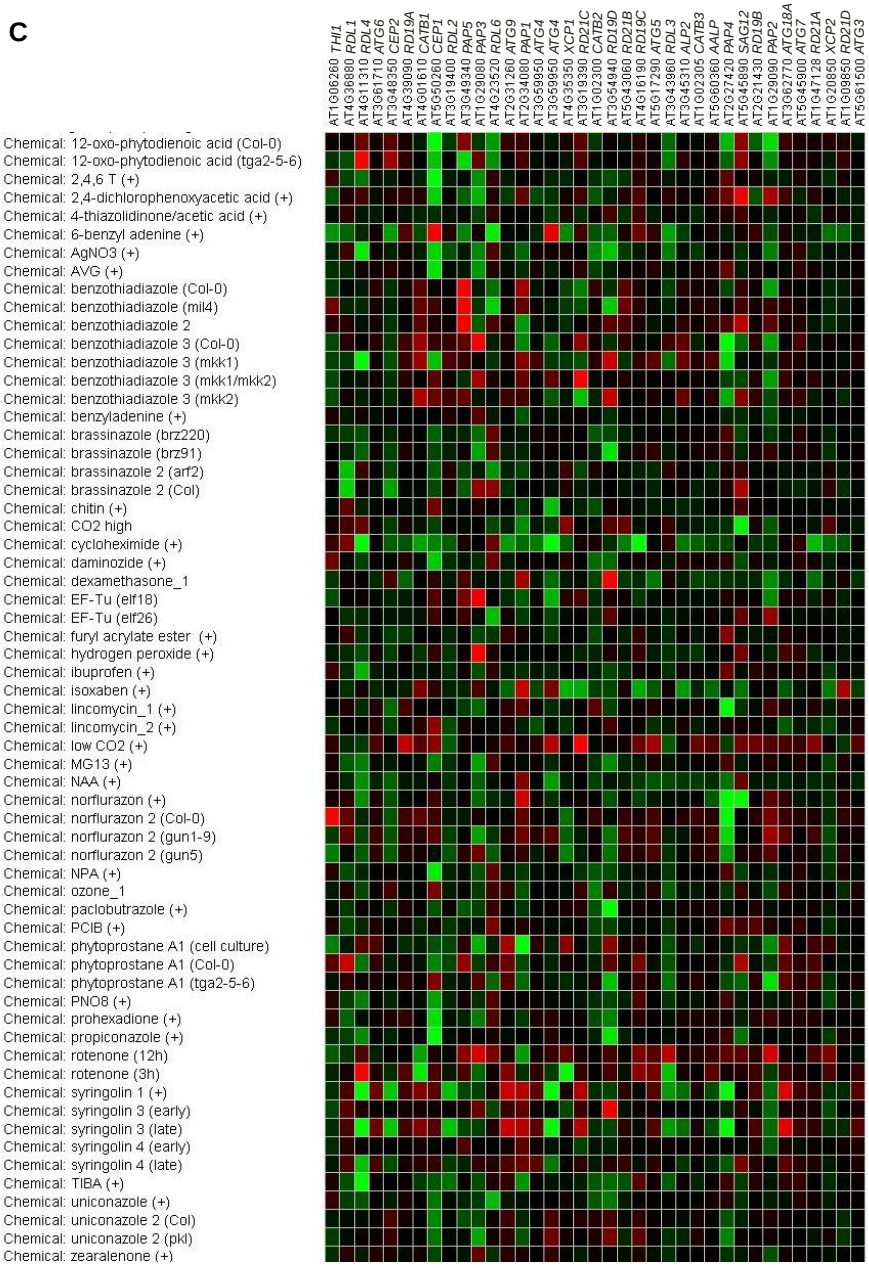
AT1G06260 THI1
AT4G36880 RDL1
AT4G11310 RDL4
AT3G61710 ATG6
AT3G48350 CEP2
AT4G39090 RD19A
AT4G01610 CATB1
AT5G50260 CEP1
AT3G19400 RDL2
AT3G49340 PAP5
AT1G29080 PAP3
AT4G23520 RDL6
AT2G31260 ATG9
AT2G34080 PAP1
AT3G59950 ATG4
AT3G59950 ATG4
AT4G35350 XCP1
AT3G19390 RD21C
AT1G02300 CATB2
AT3G54940 RD19D
AT5G43060 RD21B
AT4G16190 RD19C
AT5G17290 ATG5
AT3G43960 RDL3
AT3G45310 ALP2
AT1G02305 CATB3
AT5G60360 AALP
AT2G27420 PAP4
AT5G45890 SAG12
AT2G21430 RD19B
AT1G29090 PAP2
AT3G62770 ATG18A
AT5G45900 ATG7
AT1G47128 RD21A
AT1G20850 XCP2
AT1G09850 RD21D
AT5G61500 ATG3
Chemical: 12-oxo-phytodienoic acid (Col-0)
Chemical: 12-oxo-phytodienoic acid (tga2-5-6)
Chemical: 2,4,6 T (+)
Chemical: 2,4-dichlorophenoxyacetic acid (+)
Chemical: 4-thiazolidinone/acetic acid (+)
Chemical: 6-benzyl adenine (+)
Chemical: AgNO3 (+)
Chemical: AVG (+)
Chemical: benzothiadiazole (Col-0)
Chemical: benzothiadiazole (mil4)
Chemical: benzothiadiazole 2
Chemical: benzothiadiazole 3 (Col-0)
Chemical: benzothiadiazole 3 (mkk1)
Chemical: benzothiadiazole 3 (mkk1/mkk2)
Chemical: benzothiadiazole 3 (mkk2)
Chemical: benzyladenine (+)
Chemical: brassinazole (brz220)
Chemical: brassinazole (brz91)
Chemical: brassinazole 2 (arf2)
Chemical: brassinazole 2 (Col)
Chemical: chitin (+)
Chemical: CO2 high
Chemical: cycloheximide (+)
Chemical: daminozide (+)
Chemical: dexamethasone_1
Chemical: EF-Tu (elf18)
Chemical: EF-Tu (elf26)
Chemical: furyl acrylate ester (+)
Chemical: hydrogen peroxide (+)
Chemical: ibuprofen (+)
Chemical: isoxaben (+)
Chemical: lincomycin_1 (+)
Chemical: lincomycin_2 (+)
Chemical: low CO2 (+)
Chemical: MG13 (+)
Chemical: NAA (+)
Chemical: norflurazon (+)
Chemical: norflurazon 2 (Col-0)
Chemical: norflurazon 2 (gun1-9)
Chemical: norflurazon 2 (gun5)
Chemical: NPA (+)
Chemical: ozone_1
Chemical: paclobutrazole (+)
Chemical: PCIB (+)
Chemical: phytoprostane A1 (cell culture)
Chemical: phytoprostane A1 (Col-0)
Chemical: phytoprostane A1 (tga2-5-6)
Chemical: PNO8 (+)
Chemical: prohexadione (+)
Chemical: propiconazole (+)
Chemical: rotenone (12h)
Chemical: rotenone (3h)
Chemical: syringolin 1 (+)
Chemical: syringolin 3 (early)
Chemical: syringolin 3 (late)
Chemical: syringolin 4 (early)
Chemical: syringolin 4 (late)
Chemical: TIBA (+)
Chemical: uniconazole (+)
Chemical: uniconazole 2 (Col)
Chemical: uniconazole 2 (pkl)
Chemical: zearalenone (+)

Ahmed, S.U., Rojo, E., Kovaleva, V., Venkataraman, S., Dombrowski, J.E., Matsuoka, K., and Raikhel, N.V. (2000) The plant vacuolar sorting receptor AtELP is involved in transport of NH2-terminal propeptide-containing vacuolar proteins in *Arabidopsis thaliana*. *Journal of Cell Biology*, **149**, 1335-1344.

Alvarez, V.E., Kosec, G., Anna, C.S., Turk, V., Cazzulo, J.J., and Turk, B. (2008) Autophagy is involved in nutritional stress response and differentiation in Trypanosoma cruzi. *Journal of Biological Chemistry*, **283**, 3454-3464.

Asp, T., Bowra, S., Borg, S., and Holm, P.B. (2004) Molecular cloning, functional expression in Escherichia coli and enzymatic characterisation of a cysteine protease from white clover (Trifolium repens). *Biochimica Et Biophysica Acta-Proteins and Proteomics*, **1699**, 111-122.

Avci, U., Petzold, H.E., Ismail, I.O., Beers, E.P., and Haigler, C.H. (2008) Cysteine proteases XCP1 and XCP2 aid micro-autolysis within the intact central vacuole during xylogenesis in *Arabidopsis* roots. *Plant Journal*, **56**, 303-315.

Avrova, A.O., Stewart, H.E., De Jong, W., Heilbronn, J., Lyon, G.D., and Birch, P.R.J. (1999) A cysteine protease gene is expressed early in resistant potato interactions with Phytophthora infestans. *Molecular Plant-Microbe Interactions*, **12**, 1114-1119.

Avrova, A.O., Taleb, N., Rokka, V.M., Heilbronn, J., Campbell, E., Hein, I., Gilroy, E.M., Cardle, L., Bradshaw, J.E., Stewart, H.E., Fakim, Y.J., Loake, G., and Birch, P.R.J. (2004) Potato oxysterol binding protein and cathepsin B are rapidly up-regulated in independent defence pathways that distinguish R gene-mediated and field resistances to *Phytophthora infestans*. *Molecular Plant Pathology*, **5**, 45-56.

Azarkan, M., Dibiani, R., Baulard, C., and Baeyens-Volant, D. (2006) Effects of mechanical wounding on Carica papaya cysteine endopeptidases accumulation and activity. *Int J Biol Macromol*, **38**, 216-224.

Azevedo, C., Betsuyaku, S., Peart, J., Takahashi, A., Noel, L., Sadanandom, A., Casais, C., Parker, J., and Shirasu, K. (2006) Role of SGT1 in resistance protein accumulation in plant immunity. *Embo Journal*, **25**, 2007-2016.

Baker, M., Mackenzie, I.R., Pickering-Brown, S.M., Gass, J., Rademakers, R., Lindholm, C., Snowden, J., Adamson, J., Sadovnick, A.D., Rollinson, S., Cannon, A., Dwosh, E., Neary, D., Melquist, S., Richardson, A., Dickson, D., Berger, Z., Eriksen, J., Robinson, T., Zehr, C., Dickey, C.A., Crook, R., McGowan, E., Mann, D., Boeve, B., Feldman, H., and Hutton, M. (2006) Mutations in progranulin cause tau-negative frontotemporal dementia linked to chromosome 17. *Nature*, **442**, 916-919.

Bassham, D.C., Laporte, M., Marty, F., Moriyasu, Y., Ohsumi, Y., Olsen, L.J., and Yoshimoto, K. (2006) Autophagy in development and stress responses of plants. *Autophagy*, **2**, 2-11.

Bassham, D.C. (2007) Plant autophagy--more than a starvation response. *Curr Opin Plant Biol*, **10**, 587-593.

Bateman, A., and Bennett, H.P.J. (1998) Granulins: the structure and function of an emerging family of growth factors. *Journal of Endocrinology*, **158**, 145-151.

Beers, E.P., Jones, A.M., and Dickerman, A.W. (2004) The S8 serine, C1A cysteine and Al aspartic protease families in Arabidopsis. *Phytochemistry*, **65**, 43-58.

Belenghi, B., Acconcia, F., Trovato, M., Perazzolli, M., Bocedi, A., Polticelli, F.,

Ascenzi, P., and Delledonne, M. (2003) AtCYS1, a cystatin from Arabidopsis thaliana, suppresses hypersensitive cell death. *European Journal of Biochemistry*, **270**, 2593-2604.

Bernoux, M., Timmers, T., Jauneau, A., Briere, C., de Wit, P.J.G.M., Marco, Y., and Deslandes, L. (2008) RD19, an Arabidopsis cysteine protease required for RRS1-R-mediated resistance, is relocalized to the nucleus by the Ralstonia solanacearum PopP2 effector. *Plant Cell*, **20**, 2252-2264.

Berti, P.J., and Storer, A.C. (1995) Alignment Phylogeny of the Papain Superfamily of Cysteine Proteases. *Journal of Molecular Biology*, **246**, 273-283.

Beyene, G., Foyer, C.H., and Kunert, K.J. (2006) Two new cysteine proteinases with specific expression patterns in mature and senescent tobacco (Nicotiana tabacum L.) leaves. *J Exp Bot*, **57**, 1431-1443.

Brinig, M.M., Register, K.B., Ackermann, M.R., and Relman, D.A. (2006) Genomic features of Bordetella parapertussis clades with distinct host species specificity. *Genome Biology*, **7**, -.

Buriankova, K., Doucet-Populaire, F., Dorson, O., Gondran, A., Ghnassia, J.C., Weiser, J., and Pernodet, J.L. (2004) Molecular basis of intrinsic macrolide resistance in the Mycobacterium tuberculosis complex. *Antimicrobial Agents and Chemotherapy*, **48**, 143-150.

Cadieux, B., Chitramuthu, B.P., Baranowski, D., and Bennett, H.P.J. (2005) The zebrafish progranulin gene family and antisense transcripts. *Bmc Genomics*, **6**, -.

Carter, C., Pan, S., Zouhar, J., Avila, E.L., Girke, T., and Raikhel, N.V. (2004) The Vegetative Vacuole Proteome of Arabidopsis thaliana Reveals Predicted and Unexpected Proteins. *The Plant Cell*, **16**, 3285-3303.

Chang, Y.M., Luthe, D.S., Davis, F.M., and Williams, W.P. (2000) Influence of whorl region from resistant and susceptible corn genotypes on fall armyworm (Lepidoptera: Noctuidae) growth and development. *J Econ Entomol*, **93**, 477-483.

Chapman, S., Faulkner, C., Kaiserli, E., Garcia-Mata, C., Savenkov, E.I., Roberts, A.G., Oparka, K.J., and Christie, J.M. (2008) The photoreversible fluorescent protein iLOV outperforms GFP as a reporter of plant virus infection. *Proc Natl Acad Sci U S A*, **105**, 20038-20043.

Chen, R.D., Yu, L.X., Greer, A.F., Cheriti, H., and Tabaeizadeh, Z. (1994) Isolation of an Osmotic Stress-Induced and Abscisic-Acid-Induced Gene Encoding an Acidic Endochitinase from Lycopersicon-Chilense. *Molecular & General Genetics*, **245**, 195-202.

Chen, H.J., Huang, D.J., Hou, W.C., Liu, J.S., and Lin, Y.H. (2006) Molecular cloning and characterization of a granulin-containing cysteine protease SPCP3 from sweet potato (Ipomoea batatas) senescent leaves. *Journal of Plant Physiology*, **163**, 863-876.

Clarke, A.K. (2005) Plant proteases - an appetite for destruction. *Physiologia Plantarum*, **123**, 359-361.

Clough, S.J., and Bent, A.F. (1998) Floral dip: a simplified method for Agrobacterium-mediated transformation of *Arabidopsis thaliana*. *Plant Journal*, **16**, 735-743.

Cruts, M., Gijselinck, I., van der Zee, J., Engelborghs, S., Wils, H., Pirici, D., Rademakers, R., Vandenberghe, R., Dermaut, B., Martin, J.J., van Duijn,

C., Peeters, K., Sciot, R., Santens, P., De Pooter, T., Mattheijssens, M., Van den Broeck, M., Cuijt, I., Vennekens, K., De Deyn, P.P., Kumar-Singh, S., and Van Broeckhoven, C. (2006) Null mutations in progranulin cause ubiquitin-positive frontotemporal dementia linked to chromosome 17q21. *Nature*, **442**, 920-924.

Drake, R., John, I., Farrell, A., Cooper, W., Schuch, W., and Grierson, D. (1996) Isolation and analysis of cDNAs encoding tomato cysteine proteases expressed during leaf senescence. *Plant Molecular Biology*, **30**, 755-767.

Drenth, J., Jansoniu.Jn, Koekoek, R., Swen, H.M., and Wolthers, B.G. (1968) Structure of Papain. *Nature*, **218**, 929-&.

Eason, J.R., Ryan, D.J., Watson, L.M., Hedderley, D., Christey, M.C., Braun, R.H., and Coupe, S.A. (2005) Suppression of the cysteine protease, aleurain, delays floret senescence in *Brassica oleracea*. *Plant Molecular Biology*, **57**, 645-657.

El Moussaoui, A., Nijs, M., Paul, C., Wintjens, R., Vincentelli, J., Azarkan, M., and Looze, Y. (2001) Revisiting the enzymes stored in the laticifers of *Carica papaya* in the context of their possible participation in the plant defence mechanism. *Cell Mol Life Sci*, **58**, 556-570.

Funk, V., Kositsup, B., Zhao, C.S., and Beers, E.P. (2002) The Arabidopsis xylem peptidase XCP1 is a tracheary element vacuolar protein that may be a papain ortholog. *Plant Physiology*, **128**, 84-94.

Garcia-Lorenzo, M., Sjodin, A., Jansson, S., and Funk, C. (2006) Protease gene families in Populus and Arabidopsis. *Bmc Plant Biology*, **6**, -.

Gilroy, E.M., Hein, I., van der Hoorn, R., Boevink, P.C., Venter, E., McLellan, H., Kaffarnik, F., Hrubikova, K., Shaw, J., Holeva, M., Lopez, E.C., Borras-Hidalgo, O., Pritchard, L., Loake, G.J., Lacomme, C., and Birch, P.R.J. (2007) Involvement of cathepsin B in the plant disease resistance hypersensitive response. *Plant Journal*, **52**, 1-13.

Greenbaum, D., Medzihradszky, K.F., Burlingame, A., and Bogyo, M. (2000) Epoxide electrophiles as activity-dependent cysteine protease profiling and discovery tools. *Chemistry & Biology*, **7**, 569-581.

Grudkowska, M., and Zagdanska, B. (2004) Multifunctional role of plant cysteine proteinases. *Acta Biochimica Polonica*, **51**, 609-624.

Guerra, R.R., Kriazhev, L., Hernandez-Blazquez, F.J., and Bateman, A. (2007) Progranulin is a stress-response factor in fibroblasts subjected to hypoxia and acidosis. *Growth Factors*, **25**, 280-285.

Halls, C.E., Rogers, S.W., and Rogers, J.C. (2005) Purification of a proaleurain maturation protease. *Plant Science*, **168**, 1267-1279.

Halls, C.E., Rogers, S.W., Oufattole, M., Ostergard, O., Svensson, B., and Rogers, J.C. (2006) A Kunitz-type cysteine protease inhibitor from cauliflower and Arabidopsis. *Plant Science*, **170**, 1102-1110.

Hanaoka, H., Noda, T., Shirano, Y., Kato, T., Hayashi, H., Shibata, D., Tabata, S., and Ohsumi, Y. (2002) Leaf senescence and starvation-induced chlorosis are accelerated by the disruption of an Arabidopsis autophagy gene. *Plant Physiol*, **129**, 1181-1193.

Hanington, P.C., Brennan, L.J., Belosevic, M., and Keddie, B.A. (2008) Molecular and functional characterization of granulin-like molecules of insects. *Insect Biochemistry and Molecular Biology*, **38**, 596-603.

Hao, L., Hsiang, T., and Goodwin, P.H. (2006) Role of two cysteine proteinases in the susceptible response of *Nicotiana benthamiana* to *Colletotrichum destructivum* and the hypersensitive response to *Pseudomonas syringae* pv. *tomato*. *Plant Science*, **170**, 1001-1009.

Harrak, H., Azelmat, S., Baker, E.N., and Tabaeizadeh, Z. (2001) Isolation and characterization of a gene encoding a drought-induced cysteine protease in tomato (Lycopersicon esculentum). *Genome*, **44**, 368-374.

Hayashi, Y., Yamada, K., Shimada, T., Matsushima, R., Nishizawa, N.K., Nishimura, M., and Hara-Nishimura, I. (2001) A proteinase-storing body that prepares for cell death or stresses in the epidermal cells of *Arabidopsis*. *Plant and Cell Physiology*, **42**, 894-899.

Himber, C., Dunoyer, P., Moissiard, G., Ritzenthaler, C., and Voinnet, O. (2003) Transitivity-dependent and -independent cell-to-cell movement of RNA silencing. *Embo J*, **22**, 4523-4533.

Holwerda, B.C., and Rogers, J.C. (1992) Purification and Characterization of Aleurain - a Plant Thiol Protease Functionally Homologous to Mammalian Cathepsin-H. *Plant Physiology*, **99**, 848-855.

Inoue, Y., Suzuki, T., Hattori, M., Yoshimoto, K., Ohsumi, Y., and Moriyasu, Y. (2006) AtATG genes, homologs of yeast autophagy genes, are involved in constitutive autophagy in *Arabidopsis* root tip cells. *Plant Cell Physiol*, **47**, 1641-1652.

Jiang, B., Siregar, U., Willeford, K.O., Luthe, D.S., and Williams, W.P. (1995) Association of a 33-kilodalton cysteine proteinase found in corn callus with the inhibition of fall armyworm larval growth. *Plant Physiol*, **108**, 1631-1640.

Jovel, J., Walker, M., and Sanfacon, H. (2007) Recovery of *Nicotiana benthamiana* plants from a necrotic response induced by a nepovirus is associated with RNA silencing but not with reduced virus titer. *Journal of Virology*, **81**, 12285-12297.

Kaffarnik, F.A.R., Jones, A.M.E., Rathjen, J.P., and Peck, S.C. (2009) Effector Proteins of the Bacterial Pathogen *Pseudomonas syringae* Alter the Extracellular Proteome of the Host Plant, Arabidopsis thaliana. *Molecular & Cellular Proteomics*, **8**, 145-156.

Kalantidis, K., Tsagris, M., and Tabler, M. (2006) Spontaneous short-range silencing of a GFP transgene in *Nicotiana benthamiana* is possibly mediated by small quantities of siRNA that do not trigger systemic silencing. *Plant Journal*, **45**, 1006-1016.

Karsai, A., Muller, S., Platz, S., and Hauser, M.T. (2002) Evaluation of a homemade SYBR (R) Green I reaction mixture for real-time PCR quantification of gene expression. *Biotechniques*, **32**, 790-+.

Ketelaar, T., Voss, C., Dimmock, S.A., Thumm, M., and Hussey, P.J. (2004) Arabidopsis homologues of the autophagy protein Atg8 are a novel family of microtubule binding proteins. *Febs Letters*, **567**, 302-306.

Kikuchi, Y., Saika, H., Yuasa, K., Nagahama, M., and Tsuji, A. (2008) Isolation and Biochemical Characterization of Two Forms of RD21 from Cotyledons of Daikon Radish (Raphanus sativus). *Journal of Biochemistry*, **144**, 789-798.

Koizumi, M., Yamaguchishinozaki, K., Tsuji, H., and Shinozaki, K. (1993) Structure and Expression of 2 Genes That Encode Distinct Drought-Inducible Cysteine Proteinases in Arabidopsis-Thaliana. *Gene*, **129**, 175-182.

Konno, K., Hirayama, C., Nakamura, M., Tateishi, K., Tamura, Y., Hattori, M., and Kohno, K. (2004) Papain protects papaya trees from herbivorous insects: role of cysteine proteases in latex. *Plant J*, **37**, 370-378.

Koscianska, E., Kalantidis, K., Wypijewski, K., Sadowski, J., and Tabler, M. (2005) Analysis of RNA silencing in agroinfiltrated leaves of *Nicotiana benthamiana* and *Nicotiana tabacum*. *Plant Molecular Biology*, **59**, 647-661.

Kruger, J., Thomas, C.M., Golstein, C., Dixon, M.S., Smoker, M., Tang, S.K., Mulder, L., and Jones, J.D.G. (2002) A tomato cysteine protease required for Cf-2-dependent disease resistance and suppression of autonecrosis. *Science*, **296**, 744-747.

Kruger, J., Thomas, C.M., Golstein, C., Dixon, M.S., Smoker, M., Tang, S., Mulder, L., and Jones, J.D. (2002) A tomato cysteine protease required for Cf-2-dependent disease resistance and suppression of autonecrosis. *Science*, **296**, 744-747.

Linthorst, H.J.M., Vanderdoes, C., Vankan, J.A.L., and Bol, J.F. (1993) Nucleotide-Sequence of a Cdna Clone Encoding Tomato (Lycopersicon-Esculentum) Cysteine Proteinase. *Plant Physiology*, **101**, 705-706.

Liu, Y.L., Schiff, M., and Dinesh-Kumar, S.P. (2002) Virus-induced gene silencing in tomato. *Plant Journal*, **31**, 777-786.

Lohman, K.N., Gan, S.S., John, M.C., and Amasino, R.M. (1994) Molecular Analysis of Natural Leaf Senescence in Arabidopsis-Thaliana. *Physiologia Plantarum*, **92**, 322-328.

Lu, R., Martin-Hernandez, A.M., Peart, J.R., Malcuit, I., and Baulcombe, D.C. (2003) Virus-induced gene silencing in plants. *Methods*, **30**, 296-303.

Luderer, R., De Kock, M.J.D., Dees, R.H.L., De Wit, P.J.G.M., and Joosten, M.H.A.J. (2002) Functional analysis of cysteine residues of ECP elicitor proteins of the fungal tomato pathogen *Cladosporium fulvum*. *Molecular Plant Pathology*, **3**, 91-95.

Marshall, O.J. (2004) PerlPrimer: cross-platform, graphical primer design for standard, bisulphite and real-time PCR. *Bioinformatics*, **20**, 2471-2472.

Martinez, M., Rubio-Somoza, I., Carbonero, P., and Diaz, I. (2003) A cathepsin B-like cysteine protease gene from Hordeum vulgare (gene CatB) induced by GA in aleurone cells is under circadian control in leaves. *Journal of Experimental Botany*, **54**, 951-959.

Martinez, M., Abraham, Z., Carbonero, P., and Diaz, I. (2005) Comparative phylogenetic analysis of cystatin gene families from arabidopsis, rice and barley. *Molecular Genetics and Genomics*, **273**, 423-432.

Moutim, V., Silva, L.G., Lopes, M.T.P., Fernandes, G.W., and Salas, C.E. (1999) Spontaneous processing of peptides during coagulation of latex from *Carica papaya*. *Plant Science*, **142**, 115-121.

Noh, Y.S., and Amasino, R.M. (1999) Identification of a promoter region responsible for the senescence-specific expression of SAG12. *Plant Molecular Biology*, **41**, 181-194.

Noh, Y.S., and Amasino, R.M. (1999) Regulation of developmental senescence is conserved between *Arabidopsis* and *Brassica napus*. *Plant Molecular Biology*, **41**, 195-206.

Ondzighi, C.A., Christopher, D.A., Cho, E.J., Chang, S.C., and Staehelin, L.A.

(2008) *Arabidopsis* protein disulfide isomerase-5 inhibits cysteine proteases during trafficking to vacuoles before programmed cell death of the endothelium in developing seeds. *Plant Cell*, **20**, 2205-2220.

Otegui, M.S., Noh, Y.S., Martinez, D.E., Vila Petroff, M.G., Andrew Staehelin, L., Amasino, R.M., and Guiamet, J.J. (2005) Senescence-associated vacuoles with intense proteolytic activity develop in leaves of Arabidopsis and soybean. *Plant Journal*, **41**, 831-844.

Parker, J.E., Szabo, V., Staskawicz, B.J., Lister, C., Dean, C., Daniels, M.J., and Jones, J.D.G. (1993) Phenotypic characterization and molecular mapping of the *Arabidopsis-Thaliana* locus RPP5, determining disease resistance to *Peronospora-Parasitica*. *Plant Journal*, **4**, 821-831.

Peart, J.R., Lu, R., Sadanandom, A., Malcuit, I., Moffett, P., Brice, D.C., Schauser, L., Jaggard, D.A.W., Xiao, S.Y., Coleman, M.J., Dow, M., Jones, J.D.G., Shirasu, K., and Baulcombe, D.C. (2002) Ubiquitin ligase-associated protein SGT1 is required for host and nonhost disease resistance in plants. *Proc Natl Acad Sci U S A*, **99**, 10865-10869.

Pechan, T., Jiang, B., Steckler, D., Ye, L., Lin, L., Luthe, D.S., and Williams, W.P. (1999) Characterization of three distinct cDNA clones encoding cysteine proteinases from maize (*Zea mays L.*) callus. *Plant Mol Biol*, **40**, 111-119.

Pechan, T., Ye, L., Chang, Y., Mitra, A., Lin, L., Davis, F.M., Williams, W.P., and Luthe, D.S. (2000) A unique 33-kD cysteine proteinase accumulates in response to larval feeding in maize genotypes resistant to fall armyworm and other Lepidoptera. *Plant Cell*, **12**, 1031-1040.

Pechan, T., Cohen, A., Williams, W.P., and Luthe, D.S. (2002) Insect feeding mobilizes a unique plant defense protease that disrupts the peritrophic matrix of caterpillars. *Proc Natl Acad Sci U S A*, **99**, 13319-13323.

Pimpl, P., Hanton, S.L., Taylor, J.P., Pinto-daSilva, L.L., and Denecke, J. (2003) The GTPase ARF1p controls the sequence-specific vacuolar sorting route to the lytic vacuole. *Plant Cell*, **15**, 1242-1256.

Rawlings, N.D., Morton, F.R., and Barrett, A.J. (2006) MEROPS: the peptidase database. *Nucleic Acids Research*, **34**, D270-D272.

Rawlings, N.D., and Morton, F.R. (2008) The MEROPS batch BLAST: A tool to detect peptidases and their non-peptidase homologues in a genome. *Biochimie*, **90**, 243-259.

Rios, G., Lossow, A., Hertel, B., Breuer, F., Schaefer, S., Broich, M., Kleinow, T., Jasik, J., Winter, J., Ferrando, A., Farras, R., Panicot, M., Henriques, R., Mariaux, J.B., Oberschall, A., Molnar, G., Berendzen, K., Shukla, V., Lafos, M., Koncz, Z., Redei, G.P., Schell, J., and Koncz, C. (2002) Rapid identification of *Arabidopsis* insertion mutants by non-radioactive detection of T-DNA tagged genes. *Plant Journal*, **32**, 243-253.

Rooney, H.C., Van't Klooster, J.W., van der Hoorn, R.A., Joosten, M.H., Jones, J.D., and de Wit, P.J. (2005) Cladosporium Avr2 inhibits tomato Rcr3 protease required for Cf-2-dependent disease resistance. *Science*, **308**, 1783-1786.

Rotenberg, D., Thompson, T.S., German, T.L., and Willis, D.K. (2006) Methods for effective real-time RT-PCR analysis of virus-induced gene silencing. *Journal of Virological Methods*, **138**, 49-59.

Ruiz, M.T., Voinnet, O., and Baulcombe, D.C. (1998) Initiation and maintenance of

virus-induced gene silencing. *Plant Cell*, **10**, 937-946.

Salas, C.E., Gomes, M.T.R., Hernandez, M., and Lopes, M.T.P. (2008) Plant cysteine proteinases: Evaluation of the pharmacological activity. *Phytochemistry*, **69**, 2263-2269.

Schaffer, M.A., and Fischer, R.L. (1990) Transcriptional Activation by Heat and Cold of a Thiol Protease Gene in Tomato. *Plant Physiology*, **93**, 1486-1491.

Seay, M., Patel, S., and Dinesh-Kumar, S.P. (2006) Autophagy and plant innate immunity. *Cell Microbiol*, **8**, 899-906.

Shabab, M., Shindo, T., Gu, C., Kaschani, F., Pansuriya, T., Chintha, R., Harzen, A., Colby, T., Kamoun, S., and van der Hoorn, R.A.L. (2008) Fungal effector protein AVR2 targets diversifying defense-related Cys proteases of tomato. *Plant Cell*, **20**, 1169-1183.

Shindo, T., and Van Der Hoorn, R.A.L. (2008) Papain-like cysteine proteases: key players at molecular battlefields employed by both plants and their invaders. *Molecular Plant Pathology*, **9**, 119-125.

Solomon, M., Belenghi, B., Delledonne, M., Menachem, E., and Levine, A. (1999) The involvement of cysteine proteases and protease inhibitor genes in the regulation of programmed cell death in plants. *Plant Cell*, **11**, 431-443.

Svensson, K., Larsson, P., Johansson, D., Bystrom, M., Forsman, M., and Johansson, A. (2005) Evolution of subspecies of Francisella tularensis. *Journal of Bacteriology*, **187**, 3903-3908.

Tabaeizadeh, Z., Chamberland, H., Chen, R.D., Yu, L.X., Bellemare, G., and Lafontaine, J.G. (1995) Identification and immunolocalization of a 65 kda drought-induced protein in cultivated tomato *Lycopersicon-esculentum*. *Protoplasma*, **186**, 208-219.

Taylor, J.A., and West, D.W. (1980) The use of evan blue stain to test the survival of plant-cells after exposure to high salt and high osmotic-pressure. *Journal of Experimental Botany*, **31**, 571-576.

Taylor, M.A.J., Baker, K.C., Briggs, G.S., Connerton, I.F., Cummings, N.J., Pratt, K.A., Revell, D.F., Freedman, R.B., and Goodenough, P.W. (1995) Recombinant pro-regions from papain and papaya proteinase tv are selective high-affinity inhibitors of the mature papaya enzymes. *Protein Engineering*, **8**, 59-62.

Thomma, B.P.H.J., Eggermont, K., Penninckx, I.A.M.A., Mauch-Mani, B., Vogelsang, R., Cammue, B.P.A., and Broekaert, W.F. (1998) Separate jasmonate-dependent and salicylate-dependent defense-response pathways in Arabidopsis are essential for resistance to distinct microbial pathogens. *Proc Natl Acad Sci U S A*, **95**, 15107-15111.

Thompson, A.R., and Vierstra, R.D. (2005) Autophagic recycling: lessons from yeast help define the process in plants. *Curr Opin Plant Biol*, **8**, 165-173.

Thorlby, G., Fourrier, N., and Warren, G. (2004) The sensitive to freezing2 gene, required for freezing tolerance in *Arabidopsis thaliana*, encodes a beta-Glucosidase. *Plant Cell*, **16**, 2192-2203.

Tian, M.Y., Win, J., Song, J., van der Hoorn, R., van der Knaap, E., and Kamoun, S. (2007) A Phytophthora infestans cystatin-like protein targets a novel tomato papain-like apoplastic protease. *Plant Physiology*, **143**, 364-377.

Tolkatchev, D., Xu, P., and Ni, F. (2001) A peptide derived from the C-terminal part

of a plant cysteine protease folds into a stack of two beta-hairpins, a scaffold present in the emerging family of granulin-like growth factors. *Journal of Peptide Research*, **57**, 227-233.

Tornero, P., and Dangl, J.L. (2001) A high-throughput method for quantifying growth of phytopathogenic bacteria in Arabidopsis thaliana. *Plant Journal*, **28**, 475-481.

Trobacher, C.P., Senatore, A., and Greenwood, J.S. (2006) Masterminds or minions? Cysteine proteinases in plant programmed cell death. *Canadian Journal of Botany-Revue Canadienne De Botanique*, **84**, 651-667.

Tsuji, A., Kikuchi, Y., Ogawa, K., Saika, H., Yuasa, K., and Nagahama, M. (2008) Purification and characterization of cathepsin B-like cysteine protease from cotyledons of daikon radish, *Raphanus sativus*. *Febs Journal*, **275**, 5429-5443.

van der Hoorn, R.A.L., and Jones, J.D. (2004) The plant proteolytic machinery and its role in defence. *Current Opinion in Plant Biology*, **7**, 400-407.

van der Hoorn, R.A.L., Leeuwenburgh, M.A., Bogyo, M., Joosten, M.H.A.J., and Peck, S.C. (2004) Activity profiling of papain-like cysteine proteases in plants. *Plant Physiology*, **135**, 1170-1178.

van der Hoorn, R.A.L. (2008) Plant proteases: From phenotypes to molecular mechanisms. *Annual Review of Plant Biology*, **59**, 191-223.

Vanderauwera, S., De Block, M., van de Steene, N., de Cottet, B.V., Metzlaff, M., and Van Breusegem, F. (2007) Silencing of poly(ADP-ribose) polymerase in plants alters abiotic stress signal transduction. *Proc Natl Acad Sci U S A*, **104**, 15150-15155.

Vellios, E., Duncan, G., Brown, D., and MacFarlane, S. (2002) Immunogold localization of tobravirus 2b nematode transmission helper protein associated with virus particles. *Virology*, **300**, 118-124.

Wang, Z., Gu, C., Colby, T., Shindo, T., Balamurugan, R., Waldmann, H., Kaiser, M., and van der Hoorn, R.A.L. (2008) beta-Lactone probes identify a papain-like peptide ligase in *Arabidopsis thaliana*. *Nature Chemical Biology*, **4**, 557-563.

Wiederanders, B. (2003) Structure-function relationships in class CA1 cysteine peptidase propeptides. *Acta Biochimica Polonica*, **50**, 691-713.

Yamada, T., Ohta, H., Masuda, T., Ikeda, M., Tomita, N., Ozawa, A., Shioi, Y., and Takamiya, K. (1998) Purification of a novel type of SDS-dependent protease in maize using a monoclonal antibody. *Plant and Cell Physiology*, **39**, 106-114.

Yamada, K., Matsushima, R., Nishimura, M., and Hara-Nishimura, I. (2001) A slow maturation of a cysteine protease with a granulin domain in the vacuoles of senescing arabidopsis leaves. *Plant Physiology*, **127**, 1626-1634.

Yamada, T., Kondo, A., Ohta, H., Masuda, T., Shimada, H., and Takamiya, K. (2001) Isolation of the protease component of maize cysteine protease-cystatin complex: release of cystatin is not crucial for the activation of the cysteine protease. *Plant Cell Physiol*, **42**, 710-716.

Yamada, K., Fuji, K., Shimada, T., Nishimura, M., and Hara-Nishimura, I. (2005) Endosomal proteases facilitate the fusion of endosomes with vacuoles at the final step of the endocytotic pathway. *Plant Journal*, **41**, 888-898.

Yamada, Y., Suzuki, N.N., Hanada, T., Ichimura, Y., Kumeta, H., Fujioka, Y., Ohsumi, Y., and Inagaki, F. (2007) The crystal structure of Atg3, an

autophagy-related ubiquitin carrier protein (E2) enzyme that mediates Atg8 lipidation. *J Biol Chem*, **282**, 8036-8043.

Yamaguchishinozaki, K., Koizumi, M., Urao, S., and Shinozaki, K. (1992) Molecular-cloning and characterization of 9 CDNAs for genes that are responsive to desiccation in *Arabidopsis-thaliana* - sequence-analysis of one cdna clone that encodes a putative transmembrane channel protein. *Plant and Cell Physiology*, **33**, 217-224.

Yoshimoto, K., Hanaoka, H., Sato, S., Kato, T., Tabata, S., Noda, T., and Ohsumi, Y. (2004) Processing of ATG8s, ubiquitin-like proteins, and their deconjugation by ATG4s are essential for plant autophagy. *Plant Cell*, **16**, 2967-2983.

Zavasnik-Bergant, T., and Turk, B. (2006) Cysteine cathepsins in the immune response. *Tissue Antigens*, **67**, 349-355.

Zhao, C.S., Johnson, B.J., Kositsup, B., and Beers, E.P. (2000) Exploiting secondary growth in *Arabidopsis*. Construction of xylem and bark cDNA libraries and cloning of three xylem endopeptidases. *Plant Physiology*, **123**, 1185-1196.

Zhao, Y.F., Thilmony, R., Bender, C.L., Schaller, A., He, S.Y., and Howe, G.A. (2003) Virulence systems of *Pseudomonas syringae* pv. *tomato* promote bacterial speck disease in tomato by targeting the jasmonate signaling pathway. *Plant Journal*, **36**, 485-499.

Zimmermann, P., Hirsch-Hoffmann, M., Hennig, L., and Gruissem, W. (2004) GENEVESTIGATOR. *Arabidopsis* microarray database and analysis toolbox. *Plant Physiology*, **136**, 2621-2632.

Acknowledgments

I would like to thank Dr. Renier van der Hoorn for all the support that he provided me throughout my PhD period at the MPIZ.

Thanks to Professor Reinhard Krämer, Professor Ute Höcker and especially to Professor Paul Schulze-Lefert for accepting to be the members of my PhD examining committee.
Special thanks to Dr. Gregor Schimiz; for giving his responsibility to act as “Beisitzer” at my exam.

Big thanks to all the members of the van der Hoorn lab, past and present!
Also I have been having good support from the people all around the MPZ! Thanks for everybody!
I would like to thank my friends and former supervisor and colleagues while I was in UK. Without them most probably I would not be able to start PhD here at MPIZ.
People I met during my stay in Germany in/out of work. It was nice to get to know them and I would like to thank them too!

I really appreciate the support from my family in Japan throughout my stay in both UK and Germany. I still feel like the day I arrived in UK was not long ago. But at the same time I feel it was a long way. After almost ten years of my stay in abroad, here I have finally completed what I aimed at first!

ERKLÄRUNG

Hiermit versichere ich, Takayuki Shindo, dass ich die von mir vorgelegte Dissertation selbständig angefertigt, die benutzten Quellen und Hilfsmittel vollständig angegeben und die Stellen der Arbeit -einschließlich Tabellen, Karten und Abbildungen -, die anderen Werken im Wortlaut oder dem Sinn nach entnommen sind, in jedem Einzelfall als Entlehnung kenntlich gemacht habe; dass diese Dissertation noch keiner anderen Fakultät oder Universität zur Prüfung vorgelegen hat; dass sie - abgesehen von den auf Seite I angegebenen Teilpublikationen - noch nicht veröffentlicht worden ist sowie, dass ich eine solche Veröffentlichung vor Abschluss des Promotionsverfahrens nicht vornehmen werde. Die Bestimmungen dieser Promotionsordnung sind mir bekannt. Die von mir vorgelegte Dissertation ist von Prof. Dr. Paul Schulze-Lefert betreut worden.

LEBENSLAUF

Takayuki SHINDO

09/99 - 07/00

Qualifekationskurs zum Studium für Ausländer (Foundation course)

Universität von Essex, Essex, UK.

10/00 – 07/04

Bachelors degree in Biologie und Management

Universität von London, Royal Holloway College, Surrey, UK.

09/04 - 09/05

Masters degree in Biologie

Universität von London, Rolyal Holloway Colledge, Surrey, UK.

Abteilung Biologische Wissenschaften

Diplomarbeitsthema: “Identifying the role of the hyper-light sensitive *lyn1* mutant in Arabidopsis”

Betreuer: Dr. Enrique Lopez-Juez

SEIT 10/05

Promotionsstudent

Max Planck Institut für Züchtungforschung, Köln, Deutschland

Unabhängige van der Hoorn Arbeitsgruppe

International Max Planck Research School (I.M.P.R.S.)

Dissertationsthema: “Investigating the role of papain-like cysteine protease RD21 in plant-pathogen interactions”

Betreuer: Dr. Renier A.L. Van der Hoorn